simple, the process is expensive and time consuming, requiring roughly 3–4 years to produce any given congenic strain. To overcome this weakness, reduction of backcross generations for the establishment of congenic strains has been achieved using marker-assisted selection protocols (MASP), the so-called 'speed congenics'. The time required for deriving such congenic strains is about 1–2 years, depending on the robustness and intensiveness of the polymorphic analysis between the gene donor and recipient strains [7].

One interesting suggestion is that the breeding cycle could be shortened by superovulating and breeding juvenile females (3–4 weeks) followed by embryo transfer to mature females for production of the next generation [8]. This might shorten the generation time down to 6–7 weeks and reduce the whole congenic procedure to 1 year. This 'supersonic congenics' strategy was promising, but has not proved practical because of the limited number of oocytes that can be produced and because there are great individual differences in response to superovulation resumes.

We have attempted to develop another high-speed congenic strategy through the male germline. Recently, we have shown that the genomes of male germ cells from the first wave of spermatogenesis have the ability to support embryonic development to term. Mouse round spermatids—the youngest haploid male germ cells—appear first at 17 days after birth and can be used for the production of offspring by round spermatid injection (ROSI) into oocytes [9]. We applied this technique to the generation of congenic strains from mice with mixed genotypes bearing a transgene, a targeted KI gene or chemically induced mutant genes. At each generation, males used for backcrossing were selected based on polymorphic marker analysis: low density screening MASP using 74–176 markers distributed uniformly throughout the genome. The recipient strain for the expected genetic background was C57BL/6 for all lines of congenics. The results were very consistent and the time for producing a congenic strain was reduced significantly. Therefore, our high-speed congenic system would be very useful for the accelerated analysis of genes of interest under a defined genetic background.

Results and Discussion

Definition of the optimal male age for spermatid collection

In mice, round spermatids can be collected from 17-day-old males at the earliest and their genomes can support full term embryonic development after injection into oocytes using ROSI [9]. However, the efficiency of producing offspring using these round spermatids was extremely low (0.9%) because of their very low incidence in testicular cell suspensions (<2%). This might compromise the accurate identification of round spermatids within a limited time of oocyte micromanipulation. Therefore, we first checked the proportion of round spermatids in testicular cell suspensions from males aged 18, 20, 22 and 24 days to define the optimal age for applying ROSI. As shown in Figure 1, the percentages of round spermatids in testicular suspension increased consistently from days 18 to 24 with statistically significant differences between groups ($P<0.05$). This resulted in easier identification of round spermatids under a microscope: thus, the time required for picking up a single round spermatid was roughly 60, 15, 10 and 10 sec using cell suspensions collected at days 18, 20, 22 and 24, respectively. Therefore, we defined day 22 to be the earliest age of males that allowed the efficient identification of round spermatids in testicular cell suspensions. Testes of the mice at day 22 were smaller than in adults, but we could still collect sufficient round spermatids from a single testis to perform a ROSI experiment (about 150–250 injected oocytes).

Congenics of gene-modified strains using first-wave round spermatids

To test whether high-speed congenics using the first wave of round spermatids could be used practically, we applied the technique to three different types of gene-modified strains, TG, KI and *N*-ethyl-*N*-nitrosourea (ENU)-mutant strains. At each generation, a male used for the next application of ROSI was selected based on showing fewer heterozygous alleles by polymorphic markers that could identify the donor (DBA/2 and 129) and

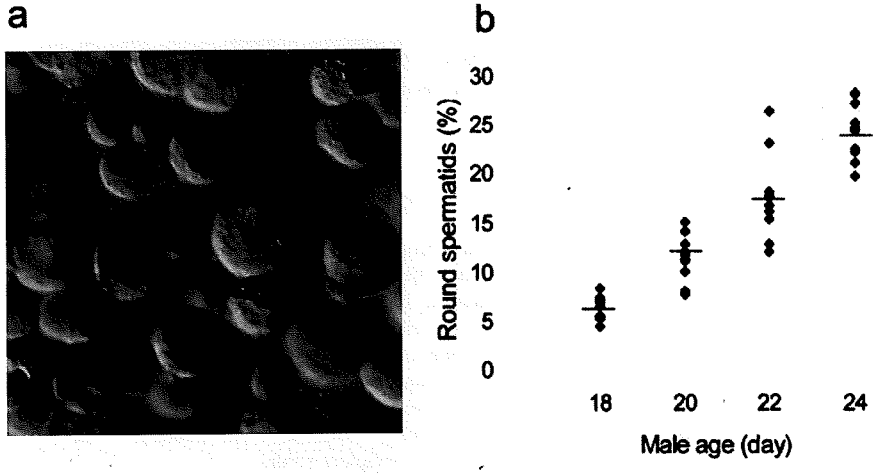

Figure 1. Definition of the optimal male age for spermatid collection. a) Representative photomicrograph of a cell suspension prepared from the testis of a male mouse at 24 days of age. Arrows indicate round spermatids, which are easily identified by a round nucleus and a high cytoplasmic/nuclear ratio. b) The proportion of round spermatids among testicular cells from 18 days to 24 days after birth. The percentages of round spermatids in testicular suspension increased consistently from days 18 to 24 ($P<0.05$ between groups). The cells were counted in two different males by two different operators. The horizontal bars indicate the average.
doi:10.1371/journal.pone.0004943.g001

recipient strains (B6Cr and B6J). Backcross ROSI was repeated until the N4 or N5 generation. After this, additional backcrossing was continued by natural mating to reduce the undetected gaps of contaminating donor alleles [10].

The *Vasa–Venus* TG strain we used was generated from embryos produced by IVF using (B6Cr×DBA/2)F1 strain oocytes and B6Cr strain spermatozoa, and maintained by full-sib mating. The N1 offspring were obtained by ICSI using a donor male at F7. As shown in Figure 2a, N5 backcross offspring were obtained on day 188 and all 74 markers were identified as B6 homozygous in one of two carrier males.

The $Ednra^{EGFP/+}$ KI strain was derived from ES cells with a (B6Cr×129^{+Tyr}/SvJcl)F1 genetic background [11]. The first N1 generation was obtained by IVF using B6Cr oocytes and spermatozoa from a chimeric mouse. All 86 markers were homozygous for B6Cr as early as at N3 (day 106; 2 out of 14 carrier males) and N4 offspring were obtained on day 151 (Figure 2b).

The ENU-induced growth differentiation factor 5 (*Gdf5*) mutant line had a mixed genetic background of B6J and DBA/2J [12]. For this combination of inbred strains, more dense polymorphic markers were available using single nucleotide polymorphism (SNP) assays as well as microsatellite genotyping (176 markers; see Materials and Methods). The N5 generation was obtained on day 190 and was 97.7% (172/176) homozygous for B6J (Figure 2c). The following N6 and N7 generations produced by IVF were 98.8% and 99.4% homozygous for B6J, respectively.

The efficiency rates in backcross breeding by ROSI in these gene-modified strains are shown in Table 1. All the modified genes could be propagated successfully into the next generations by ROSI. The male carriers finally obtained were all fertile and propagated the modified genes to the next generation by natural mating.

Significance of congenic breeding using first-wave male germ cells

Congenic strains have been used extensively for the study of mouse genetics including definition of phenotypic effects of genes on specific genetic backgrounds and identification of genes or genomic segments affecting the phenotypes of interest by quantitative trait locus (QTL) analysis. However, it takes about 2–3 years to construct a congenic strain with a level of genetic homogeneity that is reliable for research (>99% or more) [6]. To accelerate congenic breeding, MASP has been developed by taking advantage of precise information on mouse genetics [7]. Another approach for efficient congenics should be rapid generation turnover by assisted reproduction techniques. The use of immature females proposed by Behringer [8] was applied

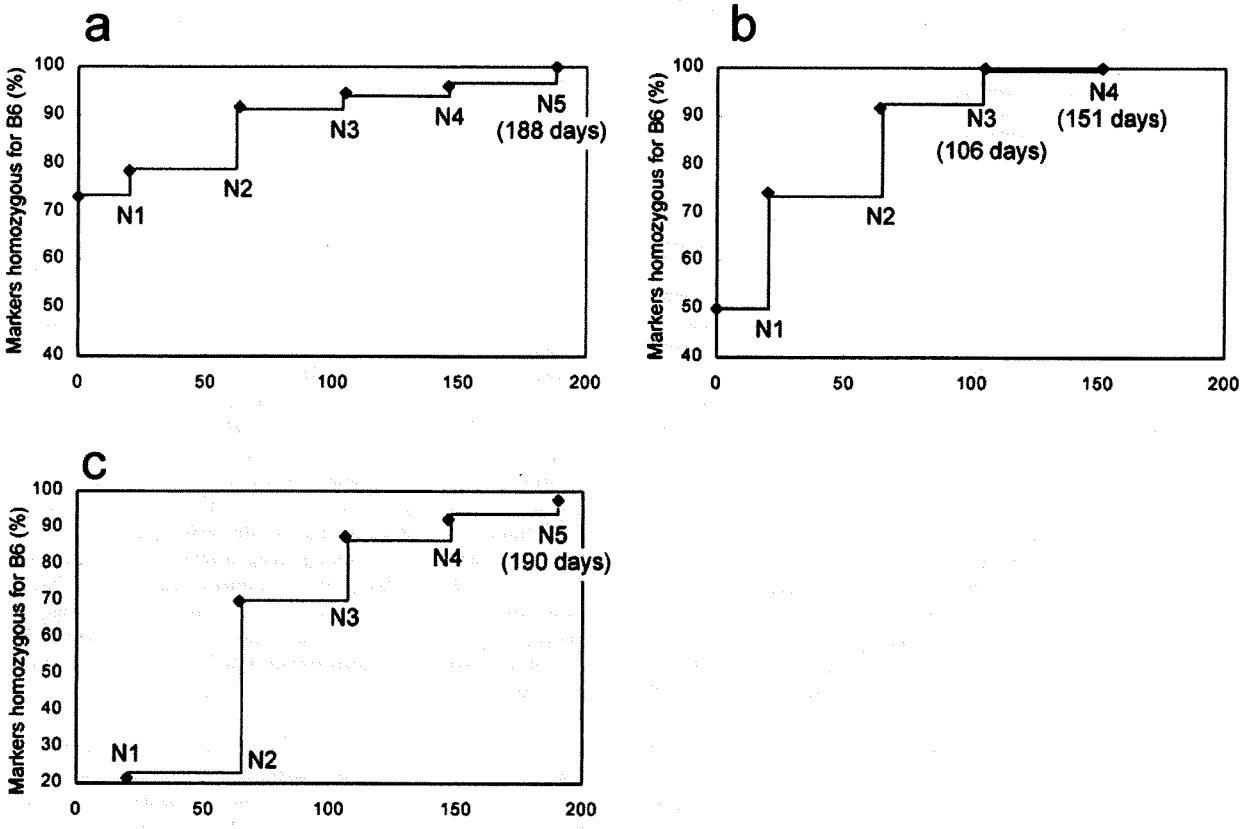

Figure 2. Time course of generation turnover and the rate of markers homozygous for the C57BL/6 (B6) type. a) *Vasa–Venus* transgenic strain. All markers (n = 74) were homozygous for B6 at N5 on day 188. b) $Ednra^{EGFP/+}$ knockin strain. All markers (n = 86) were homozygous for B6 at N3 on day 106 and N4 offspring were obtained on day 151. c) ENU-induced *Gdf5* mutant strain. The N5 generation was obtained on day 190 and was 97.7% (172/176) homozygous for B6. There were 74, 86 and 176 polymorphic markers, which identified the alleles for the C57BL/6Cr:DBA/2Cr, C57BL/6Cr:129 and C57BL/6J:DBA/2J strains, respectively. Each generation turnover was between 42 and 45 days: the age of the donor male plus the gestation period (20 days) minus the one-day overlap between them.
doi:10.1371/journal.pone.0004943.g002

Table 1. Results of congenic breeding by round spermatid injection (ROSI) in three gene-modified strains.

Strain	Generation produced	Age (day) of male used for ROSI	No. of oocyes that survived ROSI	No. (%) of oocytes that developed to 2-cells	No. of 2-cells transferred	No. (%) implanted	No. (%) born	No. (%) of males born	No. (%) of male carriers
Vasa-Venus transgenic	N1	Adult (ICSI)	16	15 (93.8)	15	10 (66.7)	5 (33.3)	5 (33.3)	5 (33.3)*
	N2	24	182	164 (90.1)	164	69 (42.1)	24 (14.6)	12 (7.3)	4 (2.4)
	N3	23	123	109 (88.6)	109	24 (22.0)	4 (3.7)	2 (1.8)	1 (0.9)
	N4	22	172	156 (90.7)	156	51 (32.7)	14 (9.0)	6 (3.8)	2 (1.3)
	N5	23	134	123 (91.8)	123	23 (18.7)	10 (8.1)	4 (3.3)	2 (1.6)
Ednra-EGFP knockin**	N1	Adult (IVF)	166	135 (81.3)	135	62 (45.9)	49 (36.3)	23 (17.0)	12 (8.9)
	N2	24	243	196 (80.7)	196	63 (32.1)	30 (15.3)	10 (5.1)	5 (2.6)
	N3	24	261	235 (90.0)	235	107 (45.5)	52 (22.1)	30 (12.8)	14 (6.0)
	N4	25	244	215 (88.1)	215	72 (33.5)	39 (18.1)	19 (8.8)	11 (5.1)
ENU-induced mutant	N1	Adult (IVF)	80	49 (61.3)	49	Not observed	26 (53.1)	14 (28.6)	3 (6.1)
	N2	25	201	158 (78.6)	158	54 (34.2)	25 (15.8)	11 (7.0)	4 (2.5)
	N3	23	208	194 (93.3)	194	68 (35.1)	26 (13.4)	12 (6.2)	7 (3.6)
	N4	22	173	127 (73.4)	127	51 (40.2)	13 (10.2)	5 (3.9)	2 (1.6)
	N5	24	216	177 (81.9)	177	91 (51.4)	34 (19.2)	10 (5.6)	4 (2.3)
Total (ROSI only)			2157	1854 (86.0)	1854	673 (36.3)	271 (14.6)	121 (6.5)	56 (3.0)
Control (C57BL/6)		22–24	467	349 (74.7)	329	133 (40.4)	49 (14.9)	26 (7.9)	

*The implantation sites were identified as the scars of decidualization at caesarian section.
**The donor male (N0) was homozygous for the transgene.
***All genetic markers tested were homozygous for the B6 mouse strain at N3.
doi:10.1371/journal.pone.0004943.t001

successfully to the derivation of a conplastic strain of rats [13]. However, there have been very few similar applications published, probably because of the limited number of oocytes produced from any one female, which may attenuate the number of carrier females in the subsequent generations. Our high-speed congenic system uses immature males as founders at each generation. Unlike females, each male can produce a large number of germ cells and multiple litters of offspring. This not only assures the safe propagation of the target gene on to the next generation, but also enables efficient selection of a male for the next round of ROSI, thus significantly shortening the time for congenics.

In this study, the advantages of our high-speed congenic strategy were shown in the KI strain, which started with a (B6Cr×129)F1 genetic background: all 86 markers were homozygous for the B6 strain as early as 106 days (N3). Apparently, it is more straightforward to use B6 ES cells for gene targeting if the B6 genetic background is required. Several B6 ES cells are available for gene targeting [14,15], and the International Knockout Consortium uses C57BL/6 ES cell lines [16]. However, B6 ES cells usually require more intense care than other 129 or hybrid ES cells to maintain their germline transmission ability during gene targeting. ES cells with hybrid genetic constitutions of B6 and 129 are easy to maintain and can be used efficiently for producing gene-targeted offspring [1,11], especially by tetraploid complementation [17]. If the gene-targeted allele is of B6 origin, it may avoid the persistence of donor genetic segments around the targeted allele during congenic production, which inevitably occurs when 129 ES cells are used. Thus, the combination of gene-targeting (B6×129)F1 ES cells and the new high-speed congenic breeding may be an alternative fast protocol to generate a B6 gene-targeting strain.

A congenic breeding strategy has also been employed extensively in laboratory rats because it is now possible to map the genetic variants and mutations that underlie complex disease-related phenotypes in this species [18,19]. ROSI is successful in some, but not all, strains of rats [20]. As the first wave of round spermatids appears in rat testes around 26 days after birth, we estimate that congenic rat strains could be generated within 7 or 8 months by using these germ cells [21].

We anticipate that the congenic strategy developed in this study might be accelerated further using male germ cells that are younger than round spermatids. This is possible theoretically, because the genomes of primary spermatocytes—premeiotic male germ cells—can support the full term development of embryos [22]. Despite many efforts to improve the technique, however, the efficiency of producing offspring using primary spermatocytes is very low [22,23]. Therefore, at present the use of round spermatids on days 22–25 may be the most practical range for efficient, rapid backcross breeding in mice. As far as we know, this is the most rapid generational turnover by sexual reproduction in mammals.

Technical issues associated with congenics by ROSI

As mentioned above, the high-speed congenic strategy we developed is very promising to produce congenic strains with desired genetic backgrounds. One of the technical issues associated with this strategy is that ROSI needs some skill and experience. However, ROSI is generally easier to perform than conventional ICSI because of the high survival rate of oocytes after injection: the diameter of injection pipettes is small and the activated oocytes used for ROSI are more resistant to the injection stimulus than nonactivated oocytes [24]. From our experience, training of three

to four consecutive weeks is enough for ROSI if the operator already has the basic technique for embryo handling. For ICSI, reliable protocol papers are available [25,26] and the same protocols can be essentially applied to ROSI. Oocytes from B6 females tend to be more sensitive to injection than those from other strains, but this problem might be overcome by using a high osmotic strength medium for manipulation on the microscope stage, if necessary. In our ROSI experiments using B6 oocytes, about 80% survived the injection whereas about 90% survived in other strains including B6D2F1, DBA/2 and 129 (unpublished).

As shown in Table 1, we consistently obtained sufficient carrier males for selection except for the N3 to N5 generations in the *Vasa–Venus* TG strain, which were affected by an accidental decline in the quality of recipient females, for reasons unknown. Based on the overall efficiency in our ROSI experiments presented in Table 1, we estimated the number of oocytes to be injected with the aim of obtaining expected number of carrier males (Table 2). These numbers of oocytes can be handled by one or two operators in a single session.

One can question if epigenetic modifications might have occurred during conception using round spermatids, because ROSI-derived preimplantation embryos have shown some disturbances in gene expression [27,28] and aberrant DNA methylation [29]. However, epigenetic errors imposed on individuals are normally erased during germ cell development and are never transmitted to the next generation by natural mating, as shown in mouse somatic cell cloning experiments [30,31]. Therefore, once mated naturally, congenic strains produced by ROSI are expected to become epigenetically indistinguishable from those produced by conventional congenic protocols.

Conclusions

The generation turnover time in mice can be shortened to about 40 days by using the first wave round spermatids as male gametes. We confirmed that this breeding strategy reduced the time required for congenesis to about half a year. This should provide the earliest opportunities for the analysis of genes of interest under a defined genetic background and for QTL mapping, which are becoming integral to biomedical research using the mouse as a model.

Materials and Methods

The origin of donor strains

The B6 substrains used in this study were B6Cr (C57BL/6CrSlc) and B6J (C57BL/6JJcl), which were purchased from CLEA Japan, Inc. (Kanagawa) and Japan SLC, Inc. (Shizuoka), respectively [32]. One mature male mouse from each strain was used as the donor of the modified gene. The TG strain we used was Tg(Mvh-Venus)1Rbrc, which was generated by DNA nuclear injection into zygotes derived from IVF using (B6Cr×DBA/2)F1 oocytes and B6Cr spermatozoa. The *Mvh-Venus* gene clearly shows the germline origin of living cells by green fluorescence because of the highly specific expression of the *Mvh* (mouse vasa homologue) gene [33]. The strain was maintained by full-sib mating. An F7 male homozygous for the transgene was used as the donor.

The KI line we used was the $Ednra^{EGFP/+}$ strain carrying the reporter gene for enhanced green fluorescence protein (EGFP) that had been knocked into the *Ednra* (endothelin receptor type A) locus by recombinase-mediated cassette exchange based on the Cre-lox system [11]. The gene-targeted ES cells had the (B6Cr×129^{+Tg}/SvJcl)F1 genotype. Chimeric embryos were produced by injection of ES cells into ICR blastocysts and they were transferred into pseudopregnant ICR females. A chimeric male thus obtained were used for producing N1 by conventional IVF using B6Cr oocytes.

The ENU-induced mutant strain we used carried a point mutation at the *Gdf5* locus. This mutation causes an amino acid substitution in a highly conserved region of the active signaling domain of the GDF5 (growth differentiation factor 5) protein, leading to impaired joint formation and osteoarthritis [12]. The donor male had a mixed genetic background of B6J and DBA/2 because the strain was generated from a cross of an ENU-mutagenized B6J male and a wild-type DBA/2 female.

Offspring that carried modified genes were genotyped at each generation by polymerase chain reaction (PCR) amplification with specific primers for the given TG strain [34], by specific green fluorescence over the body for the KI strain and by PCR-based sequencing for the ENU mutant strain [12].

Table 2. The numbers of superovulated females and oocytes required for obtaining selectable numbers of carrier males, as estimated from the data in Table 1.

Females superovulated (25–30 oocytes per female)	4 to 5	6 to 7	7 to 8
Oocytes injected	125	167	208
Oocytes survived (80% per oocytes injected)	100	133	167
2-cells transferred (80% per oocytes survived)	80	107	133
Birth (15% per 2-cells transferred)	12	16	20
Males (50% per birth)	6	8	10
Carrier males (50% per males)	3	4	5

doi:10.1371/journal.pone.0004943.t002

Collection of oocytes

Female B6Cr or B6J strain mice (7–10 weeks old) were each injected with 7.5 units of equine chorionic gonadotropin followed by injection of 7.5 units of human chorionic gonadotropin (hCG) 48 h later. Mature oocytes were collected from the oviducts 15–17 h after hCG injection and were freed from cumulus cells by treatment with 0.1% hyaluronidase in CZB medium [35]. The oocytes were transferred to fresh CZB medium and incubated at 37°C in an atmosphere of 5% CO_2 in air for up to 90 min before ROSI.

Preparation of testicular cell suspensions

Spermatogenic cells were prepared mechanically as described for hamsters [36]. Briefly, testes were removed from 18- to 25-day-old males and placed in erythrocyte-lysing buffer (155 mM NH_4Cl/10 mM $KHCO_3$/2 mM EDTA, pH 7.2). For the first series of experiments to identify the optimal age of males for donors, we used ICR males; as far as we examined there were no strain-dependent differences in the timing of the first wave of spermatogenesis. The tunica albuginea was removed and the seminiferous tubule masses were transferred into cold (4°C) Dulbecco's phosphate buffered saline (PBS) supplemented with 5.6 mM glucose, 5.4 mM sodium lactate and 0.1 mg/ml of polyvinyl alcohol (polyvinylpyrrolidone, PVP, in the original report) (GL-PBS) [36]. The seminiferous tubules were cut into small pieces and pipetted gently to disperse spermatogenic cells into the GL-PBS. Then, the cell suspension was filtered through a 38-μm nylon mesh and washed three times by centrifugation (200 *g* for 4 min). To define the optimal male age for spermatid collection, we first examined the proportion of round spermatids in

cell suspensions collected from two males aged at 18, 20, 22, or 24 days. The percentages of round spermatids were analyzed using arcsine transformation, followed by one-way ANOVA analysis and a *post-hoc* procedure using Scheffe's test for multiple comparisons.

ROSI

ROSI was performed using a Piezo-driven micromanipulator (Prime Tech Ltd., Ibaraki, Japan) as described [37,38]. The cover of a plastic dish (Falcon no. 1006; Becton Dickinson, Franklin Lakes, NJ) was used as a microinjection chamber. Several small drops (~4 μl) of Hepes-buffered CZB with or without 10% PVP were placed on the bottom and covered with mineral oil. Spermatogenic cells were placed in one of the PVP droplets. Before injection of the nuclei of round spermatids, oocytes were activated by treatment with Ca^{2+}-free CZB medium containing 2.5 mM $SrCl_2$ for 20 min at 37°C. Oocytes reaching telophase II at 40–90 min after onset of activation treatment were each injected with a round spermatid. They were kept in Hepes-CZB at room temperature (24°C) for ~10 min before culture in CZB at 37°C under 5% CO_2 in air.

Embryo culture and transfer

Embryos that reached the 2-cell stage by 24 h of culture in CZB were transferred into the oviducts of pseudopregnant ICR strain females (8–12 weeks old) on the day after mating (day 0.5). On day 19.5, recipient females were killed and their uteri were examined for live term fetuses. These were nursed by lactating ICR foster females. The day of birth was designated day 0.5 for newborns.

Care and use of animals

All procedures described here were reviewed and approved by the Animal Experimental Committee at the RIKEN Institute.

Genotyping for MASP

Tail clips about 0.3 cm long were collected for DNA extraction, using the Wizard Genomic DNA Purification Kit (Promega, Madison, WI) and the DNeasy 96 Blood & Tissue Kit (#69582; QIAGEN GmbH, Hilden, Germany) according to the manufacturers' instructions. Microsatellite genotyping was carried out by PCR for simple sequence length polymorphisms (SSLP) using microsatellite markers. The microsatellite markers were selected out of sequence length polymorphisms between B6 and DBA/2 and B6 and 129 strains (Mekada et al., unpublished data) (Tables S1 and S2). PCR execution was performed using the QIAGEN Multiplex PCR kit (#206143; QIAGEN GmbH) and the length polymorphism was detected by agarose gel electrophoresis. Map locations and primer sequences of the microsatellite loci were used according to the Mouse Genome Informatics (MGI) of the Jackson Laboratory, USA, and Mouse Microsatellite Data Base of Japan (MMDBJ).

SNP genotyping was carried out using a TaqMan Minor Groove Binding (MGB) assay (Applied Biosystems, Foster City, CA). TaqMan MGB probe sets were designed based on SNP polymorphism between C57BL/6J and DBA/2J (Table S3). PCR execution was performed using TaqMan Genotyping Master Mix (#4371353; Applied Biosystems). SNP polymorphisms were detected using an ABI PRISM 7900HT Sequence Detection System (Applied Biosystems).

Supporting Information

Table S1 Variation alleles between C57BL/6 and DBA/2 mouse strains.
Found at: doi:10.1371/journal.pone.0004943.s001 (0.02 MB XLS)

Table S2 Variation alleles between C57BL/6 and 129 mouse strains.
Found at: doi:10.1371/journal.pone.0004943.s002 (0.02 MB XLS)

Table S3 The SNPs information that designed the TaqMan MGB probe sets.
Found at: doi:10.1371/journal.pone.0004943.s003 (0.02 MB XLS)

Acknowledgments

We would like to thank Drs. Masumi Hirabayashi and Hiromi Miki for discussion on round spermatid injection techniques and Dr. Tomokazu Amano for the genetic information on the (B6×129)F1 ES cell line.

Author Contributions

Conceived and designed the experiments: NO AO. Performed the experiments: NO KI MH IM KM KM. Analyzed the data: NO IM SW AO. Contributed reagents/materials/analysis tools: TS NM KM AY KA YK. Wrote the paper: NO IM SW AO.

References

1. Glaser S, Anastassiadis K, Stewart AF (2005) Current issues in mouse genome engineering. Nat Genet 37: 1187–1193.
2. Yoshiki A, Moriwaki K (2006) Mouse phenome research: implications of genetic background. ILAR J 47: 94–102.
3. Eisener Dorman AF, Lawrence DA, Bolivar VJ (2008) Cautionary insights on knockout mouse studies: The gene or not the gene? Brain Behav Immun, In press.
4. Simpson EM, Linder CC, Sargent EE, Davisson MT, Mobraaten LE, et al. (1997) Genetic variation among 129 substrains and its importance for targeted mutagenesis in mice. Nat Genet 16: 19–27.
5. Livy DJ, Wahlsten D (1991) Tests of genetic allelism between four inbred mouse strains with absent corpus callosum. J Hered 82: 459–464.
6. Flaherty L (1981) Congenic strains. In: Foster HL, Small JD, Fox JG, eds. The Mouse in Biomedical Research (Vol. 1). New York: Academic Press. pp 215–222.
7. Markel P, Shu P, Ebeling C, Carlson GA, Nagle DL, et al. (1997) Theoretical and empirical issues for marker-assisted breeding of congenic mouse strains. Nat Genet 17: 280–284.
8. Behringer R (1998) Supersonic congenics? Nat Genet 18: 108.
9. Miki H, Lee J, Inoue K, Ogonuki N, Noguchi Y, et al. (2004) Microinsemination with first-wave round spermatids from immature male mice. J Reprod Dev 50: 131–137.
10. Armstrong NJ, Brodnicki TC, Speed TP (2006) Mind the gap: analysis of marker-assisted breeding strategies for inbred mouse strains. Mamm Genome 17: 273–287.
11. Sato T, Kawamura Y, Asai R, Amano T, Uchijima Y, et al. (2008) Recombinase-mediated cassette exchange reveals the selective use of Gq/G11-dependent and -independent endothelin 1/endothelin type A receptor signaling in pharyngeal arch development. Development 135: 755–765.
12. Masuya H, Nishida K, Furuichi T, Toki H, Nishimura G, et al. (2007) A novel dominant-negative mutation in Gdf5 generated by ENU mutagenesis impairs joint formation and causes osteoarthritis in mice. Hum Mol Genet 16: 2366–2375.
13. Pravenec M, Hyakukoku M, Houstek J, Zidek V, Landa V, et al. (2007) Direct linkage of mitochondrial genome variation to risk factors for type 2 diabetes in conplastic strains. Genome Res 17: 1319–1326.
14. Seong E, Saunders TL, Stewart CL, Burmeister M (2004) To knockout in 129 or in C57BL/6: that is the question. Trends Genet 20: 59–62.
15. Pacholczyk G, Suhag R, Mazurek M, Dederscheck SM, Koni PA (2008) Generation of C57BL/6 knockout mice using C3H×BALB/c blastocysts. Biotechniques 44: 413–416.
16. Collins FS, Rossant J, Wurst W (2007) A mouse for all reasons. Cell 128: 9–13.
17. George SH, Gertsenstein M, Vintersten K, Korets Smith E, Murphy J, Stevens ME, Haigh JJ, Nagy A (2007) Developmental and adult phenotyping

directly from mutant embryonic stem cells. Proc Natl Acad Sci U S A 104: 4455–4460.
18. Aitman TJ, Critser JK, Cuppen E, Dominiczak A, Fernandez-Suarez XM, et al. (2008) Progress and prospects in rat genetics: a community view. Nat Genet 40: 516–522.
19. Saar K, Beck A, Bihoreau MT, Birney E, Brocklebank D, et al. (2008) SNP and haplotype mapping for genetic analysis in the rat. Nat Genet 40: 560–566.
20. Hirabayashi M, Kato M, Aoto T, Ueda M, Hochi S (2002) Rescue of infertile transgenic rat lines by intracytoplasmic injection of cryopreserved round spermatids. Mol Reprod Dev 62: 295–299.
21. Jahnukainen K, Chrysis D, Hou M, Parvinen M, Eksborg S, et al. (2004) Increased apoptosis occurring during the first wave of spermatogenesis is stage-specific and primarily affects midpachytene spermatocytes in the rat testis. Biol Reprod 70: 290–296.
22. Ogura A, Suzuki O, Tanemura K, Mochida K, Kobayashi Y, et al. (1998) Development of normal mice from metaphase I oocytes fertilized with primary spermatocytes. Proc Natl Acad Sci U S A 95: 5611–5615.
23. Miki H, Ogonuki N, Inoue K, Baba T, Ogura A (2006) Improvement of cumulus-free oocyte maturation in vitro and its application to microinsemination with primary spermatocytes in mice. J Reprod Dev 52: 239–248.
24. Miki H, Hirose M, Ogonuki N, Inoue K, Kezuka F, et al. Efficient production of androgenetic embryos by round spermatid injection. Genesis, In press.
25. Nagy A, Gertsenstein M, Vintersten K, Behringer R (2003) Manipulating the Mouse Embryo: A Laboratory Manual (3rd edition). New York: Cold Spring Harbor Laboratory Press. 565 p.
26. Yoshida N, Perry AC (2007) Piezo-actuated mouse intracytoplasmic sperm injection (ICSI). Nat Protoc 2: 296–304.
27. Hayashi S, Yang J, Christenson L, Yanagimachi R, Hecht NB (2003) Mouse preimplantation embryos developed from oocytes injected with round spermatids or spermatozoa have similar but distinct patterns of early messenger RNA expression. Biol Reprod 69: 1170–1176.
28. Ziyyat A, Lefevre A (2001) Differential gene expression in pre-implantation embryos from mouse oocytes injected with round spermatids or spermatozoa. Hum Reprod 16: 1449–1456.
29. Kishigami S, Van Thuan N, Hikichi T, Ohta H, Wakayama S, et al. (2006) Epigenetic abnormalities of the mouse paternal zygotic genome associated with microinsemination of round spermatids. Dev Biol 289: 195–205.
30. Shimozawa N, Ono Y, Kimoto S, Hioki K, Araki Y, et al. (2002) Abnormalities in cloned mice are not transmitted to the progeny. Genesis 34: 203–207.
31. Tamashiro KLK, Wakayama T, Akutsu H, Yamazaki Y, Lachey JL, et al. (2002) Cloned mice have an obese phenotype not transmitted to their offspring. Nat Med 8: 262–267.
32. Mekada K, Abe K, Murakami A, Nakamura S, Nakata H, Moriwaki K, Obata Y, Yoshiki A (2009) Genetic differences among C57BL/6 substrains. Exp Anim, In press.
33. Fujiwara Y, Komiya T, Kawabata H, Sato M, Fujimoto H, et al. (1994) Isolation of a DEAD-family protein gene that encodes a murine homolog of Drosophila vasa and its specific expression in germ cell lineage. Proc Natl Acad Sci U S A 91: 12258–12262.
34. Nagai T, Ibata K, Park ES, Kubota M, Mikoshiba K, et al. (2002) A variant of yellow fluorescent protein with fast and efficient maturation for cell-biological applications. Nat Biotechnol 20: 87–90.
35. Chatot CL, Ziomek CA, Bavister BD, Lewis JL, Torres I (1989) An improved culture medium supports development of random-bred 1-cell mouse embryos in vitro. J Reprod Fertil 86: 679–688.
36. Ogura A, Yanagimachi R (1993) Round spermatid nuclei injected into hamster oocytes form pronuclei and participate in syngamy. Biol Reprod 48: 219–225.
37. Kimura Y, Yanagimachi R (1995) Mouse oocytes injected with testicular spermatozoa or round spermatids can develop into normal offspring. Development 121: 2397–2405.
38. Ogonuki N, Mochida K, Miki H, Inoue K, Fray M, et al. (2006) Spermatozoa and spermatids retrieved from frozen reproductive organs or frozen whole bodies of male mice can produce normal offspring. Proc Natl Acad Sci U S A 103: 13098–13103.

Placenta 30 (2009) 543–546

Contents lists available at ScienceDirect

Placenta

journal homepage: www.elsevier.com/locate/placenta

Short Communication

Embryonic Rather than Extraembryonic Tissues Have More Impact on the Development of Placental Hyperplasia in Cloned Mice

H. Miki [a,1], N. Wakisaka [a,1], K. Inoue [a,b,1], N. Ogonuki [a], M. Mori [c], J.-M. Kim [a], A. Ohta [c], A. Ogura [a,b,d,*]

[a] Bioresource Center, RIKEN, Tsukuba, Ibaraki 305-0074, Japan
[b] Graduate School of Life and Environmental Science, University of Tsukuba, Tsukuba, Ibaraki 305-8572, Japan
[c] Department of Life Science, School of Agriculture, Meiji University, Kawasaki, Japan
[d] The Center for Disease Biology and Integrative Medicine, Faculty of Medicine, University of Tokyo, Bunkyo-ku, Tokyo, Japan

ARTICLE INFO

Article history:
Accepted 10 March 2009

Keywords:
Hyperplasia
Nuclear transfer
Cloning
Chimera
Tetraploid

ABSTRACT

Somatic cell cloning by nuclear transfer (NT) in mice is associated with hyperplastic placentas at term. To dissect the effects of embryonic and extraembryonic tissues on this clone-associated phenotype, we constructed diploid (2*n*) fused with (⇔) tetraploid (4*n*) chimeras from NT- and fertilization-derived (FD) embryos. Generally, the 4*n* cells contributed efficiently to all the extraembryonic tissues but not to the embryo itself. Embryos constructed by 2*n* NT ⇔ 4*n* FD aggregation developed hyperplastic placentas (0.33 ± 0.22 g) with a predominant contribution by NT-derived cells. Even when the population of FD-derived cells in placentas was increased using multiple FD embryos (up to four) for aggregation, most placentas remained hyperplastic (0.36 ± 0.13 g). By contrast, placentas of the reciprocal combination, 2*n* FD ⇔ 4*n* NT, were less hyperplastic (0.15 ± 0.02 g). These nearly normal-looking placentas had a large proportion of NT-derived cells. Thus, embryonic rather than extraembryonic tissues had more impact on the onset of placental hyperplasia, and that the abnormal placentation in clones occurs in a noncell-autonomous manner. These findings suggest that for improvement of cloning efficiency we should understand the mechanisms regulating placentation, especially those of embryonic origin that might control the proliferation of trophoblastic lineage cells.

1. Introduction

The high rate of pregnancy loss following somatic cell nuclear transfer (NT) in mammals is often associated with functional defects of the placenta [1]. Even fetuses that reach term occasionally have placentas with morphological anomalies that are specific to each cloned species. In cloned mice, the placenta at term is characterized by a type of hyperplasia caused by enlargement of the spongiotrophoblast (ST) layer (junctional zone) and an increase in glycogen-bearing trophoblastic cells [2,3]. The unique nature of this placental hyperplasia is the highly consistent morphology among different donor cell types and mouse strains, except for the 129 strain [4–8]. Interestingly, placental hyperplasia is also found under certain experimental conditions including inter(sub)species hybridization [9], sperm injection following the injection of somatic cell cytoplasm into an oocyte [10] and deletion of the *Esx1* gene [11]. The gross morphology as well as ultrastructural features is common to all these mouse models of placental hyperplasia [12]. Therefore, its possible etiological cascade has been an attractive subject of research in respect of the interactions between different cell types. However, despite many efforts of genetic and epigenetic analyses, no key molecules or genes have been identified so far.

Analysis of chimeric embryos can offer a complementary experimental approach to the assessment of phenotypes. As cells from tetraploid embryos are known to give rise mainly to the extraembryonic primitive endoderm and trophectoderm, diploid fused with (⇔) tetraploid chimeras can be used to distinguish whether a patterning defect is caused by the embryonic and/or extraembryonic defects [13]. Therefore, it would be interesting to see whether fertilization-derived (FD) tetraploid embryos can rescue NT embryos with placental abnormalities. However, according to Jouneau et al. [14], the majority of diploid NT ⇔ tetraploid FD embryos had the extraembryonic ectoderm composed of NT-derived tissues at the early postimplantation stages (day 7). This finding indicates that the tetraploid cells had been supplanted by NT-derived cells, unlike those in other tetraploid complementary experiments reported previously [13].

* Corresponding author. Bioresource Center, RIKEN, Tsukuba, Ibaraki 305-0074, Japan. Tel.: +81 29 836 9165.
E-mail address: ogura@rtc.riken.go.jp (A. Ogura).
[1] HM, NW, and KI contributed equally to this work.

0143-4004/$ – see front matter © 2009 Elsevier Ltd. All rights reserved.
doi:10.1016/j.placenta.2009.03.006

To further define the role of clone-derived lineages in hyperplastic placentas, we analyzed term placentas from chimeras produced by aggregation of a single diploid embryo and multiple tetraploid embryos, which might increase the contribution of tetraploid derivatives to the placental tissues. Intriguingly, our results suggested that the embryonic rather than extraembryonic tissues had more impact on the placental size and that the abnormal placentation in clones occurs in a noncell-autonomous manner.

2. Materials and methods

2.1. Embryos

NT embryos were prepared by injecting cumulus cell nuclei from mouse strain B6D2F1 into enucleated B6D2F1 oocytes as reported [5,15]. FD embryos were prepared by conventional in vitro fertilization (IVF) using B6D2F1 oocytes and C57BL/6 or B6D2F1 spermatozoa [16]. Some IVF experiments were conducted using spermatozoa from transgenic males (C57BL/6-Tg(CAG-EGFP)C14-Y01-FM131Osb), which express the gene for green fluorescent protein (GFP) in their whole body [17]. As they were homozygous for the GFP gene, placental tissues derived from their sperm were all positive for the green fluorescence. The numbers of placentas analyzed for the GFP localization are shown in Table 1. Embryos were cultured in KSOM [18] medium at 37 °C under 5% CO_2 in air. Tetraploid embryos were produced by fusing the blastomeres of 2-cell diploid embryos, as described previously [19]. Electrofusion was induced by a DC pulse (150 V/mm, 20 ms) with pre- and post-AC pulses (15 V/cm, 2 MHz, about 10–20 s) using the cell fusion apparatus SSH-1 and electrode chamber FTC-02 (Shimadzu, Kyoto, Japan) in fusion medium (300 nM mannitol, 100 mM $MgSO_4$, 0.5 mg/ml polyvinyl alcohol and 3 mg/ml bovine serum albumin).

2.2. Generation of aggregation chimeras and embryo transfer

An 8-cell diploid embryo and one to four 4-cell tetraploid embryo(s) were aggregated at about 80 h in culture. The zona pellucida was removed by a short exposure to acidified Tyrode's medium (Sigma–Aldrich, St Louis, MO, USA). These embryos were nestled in a hole of the plastic dish made by a darning needle (BLS, Budapest, Hungary) and cultured overnight. Successfully aggregated embryos at the morula or blastocyst stage were transferred into the uteri of day 2.5 pseudopregnant ICR strain females. Full term conceptuses were delivered and the implantation sites were recorded on day 19.5 by Cesarean section.

2.3. Histological analysis

The placentas were fixed immediately with a commercial solution (Sakura Finetek, Tokyo, Japan) overnight at 4 °C. For preparing paraffin-embedded sections, the fixed tissues were processed as described previously [20]. For preparing frozen sections, the fixed tissues were immersed in a gradual series of 10–30% sucrose–PBS solutions, embedded in Tissue-Tek OCT compound (Sakura Finetek). For in situ hybridization, 8 μm thick sections either from paraffin-embedded or from frozen tissues were processed and examined under a light microscope as described [12]. In situ hybridization was performed using an antisense digoxigenin-labeled *Tpbpa* riboprobe for visualization of the ST layer. For localizing GFP-bearing cells, frozen sections (20 μm thick) were observed using a fluorescent microscope (E800, Nikon, Tokyo, Japan). For their accurate localization, the thickness of the section, the objective lens used (Plan Apo 4×), the exposure time (20 s) and all other parameters were kept constant throughout the experiments.

2.4. Statistical analysis

Experiments were repeated at least twice for each chimeric embryo group. The implantation rates, birth rates and placental weights were analyzed using Bonferroni/Dunn tests for multiple comparisons. The percentages of implantation and birth were subjected to arcsine transformation before analysis.

3. Results and discussion

Chimeric embryos were constructed by aggregating a single NT embryo with a single or multiple (two to four) FD embryos. They are referred to as 2*n* NT ⇔ (number) × 4*n* FD embryos hereafter. We also constructed 2*n* FD ⇔ 1 × 4*n* NT embryos and 2*n* non-chimeric FD embryos. The developmental ability of these chimeric embryos is shown in Table 1. Cloned (or clonal [21]) mice were born in groups of chimeric embryos from 1×, 3× and 4 × 4*n* FD aggregation embryos (Table 1). Multiplying 4*n* FD embryos for aggregation did not improve the development of clones; the full term development rate of 0–6% was within the usual range of mouse cloning efficiency using B6D2F1 strain cumulus cells [5,15]. By contrast, 2*n* FD ⇔ 4*n* NT embryos developed better, about 18% reaching term and normal birth.

The placentas from 2*n* NT ⇔ 4*n* FD chimeric embryos were larger than the 2*n* FD ⇔ 4*n* NT chimeric embryos ($P < 0.05$; Table 1). They showed the hyperplastic histology typical of mouse clones: an irregular boundary between the labyrinthine and ST layers, enlarged ST layers and increased number of glycogen-bearing cells (Fig. 1A). Placentas from embryos aggregated with multiple 4*n* FD embryos also showed the same hyperplastic structure (Fig. 1D). The average weight of the placentas derived from multiple 4*n* FD embryos (three 3× and three 4×) was 0.36 ± 0.13 g. In contrast, the placentas from 2*n* FD ⇔ 4*n* NT embryos were significantly smaller and showed only occasional histological alterations including an irregular boundary between the two layers (Fig. 1G). Their average weight was not significantly different from that of 2*n* FD ⇔ 4*n* FD embryos (Table 1), and their histological appearances were indistinguishable from each other (Fig. 1M). These findings indicate that the origin of the 4*n* cells have no significant effect on the placental morphology. Although not statistically different, aggregation of 2*n* ⇔ 4*n* embryos itself induced slight increase of the placental size (Table 1).

To discriminate the origins of the cells composing chimeric placentas, we observed the GFP fluorescence of FD-derived cells using fluorescent microscopy. As shown in Fig. 1B, placentas from 2*n* NT ⇔ 1 × 4*n* FD embryos were predominantly composed of nonfluorescent cells, indicating that the 4*n* FD cells had been supplanted by the NT cells during placentation. As the number of 4*n* FD embryos for aggregation was increased, the population of FD cells increased in the placental tissues. Even placentas of mostly FD cell origin had hyperplastic features (Fig. 1E). The intensity of the GFP fluorescence in their labyrinthine layer seemed weaker than that of the non-chimeric placentas (see Fig. 1K). This was probably because

Table 1
Development of chemeric embryos following embryo transfer and the weight of their term placentas.

Origin of embryos (2*n*:4*n*)	No. embryos aggregated (2*n*:4*n*)	No. of embryos transferred	No. (%) embryos implanted	No. (%) embryos that reached term	Placental weight (g ± S.E.)	No. of placentas observed for GPF localization
NT:FD	1:1	287	82 (29)	7 (2)[a]	0.33 ± 0.22[b]	5
	1:2	65	31 (48)	0 (0)		
	1:3	48	31 (65)	3 (6)	0.22 ± 0.03	3
	1:4	68	43 (63)	3 (4)	0.45 ± 0.22[b]	3
FD:NT	1:1	152	55 (36)	27 (18)[a']	0.15 ± 0.02[b']	3
FD:FD	1:1	21	7 (33)	7 (33)	0.17 ± 0.03[b']	
FD only	–	65	33 (51)	29 (45)	0.09 ± 0.02[b'c]	
NT only	–	175	90 (51)	9 (5)	0.30 ± 0.03[c']	

FD, Fertilization-derived embryos; NT, Nuclear transfer-derived embryos. [a,a']; [b,b']; [c,c'] $P < 0.05$ (Bonferroni/Dunn).

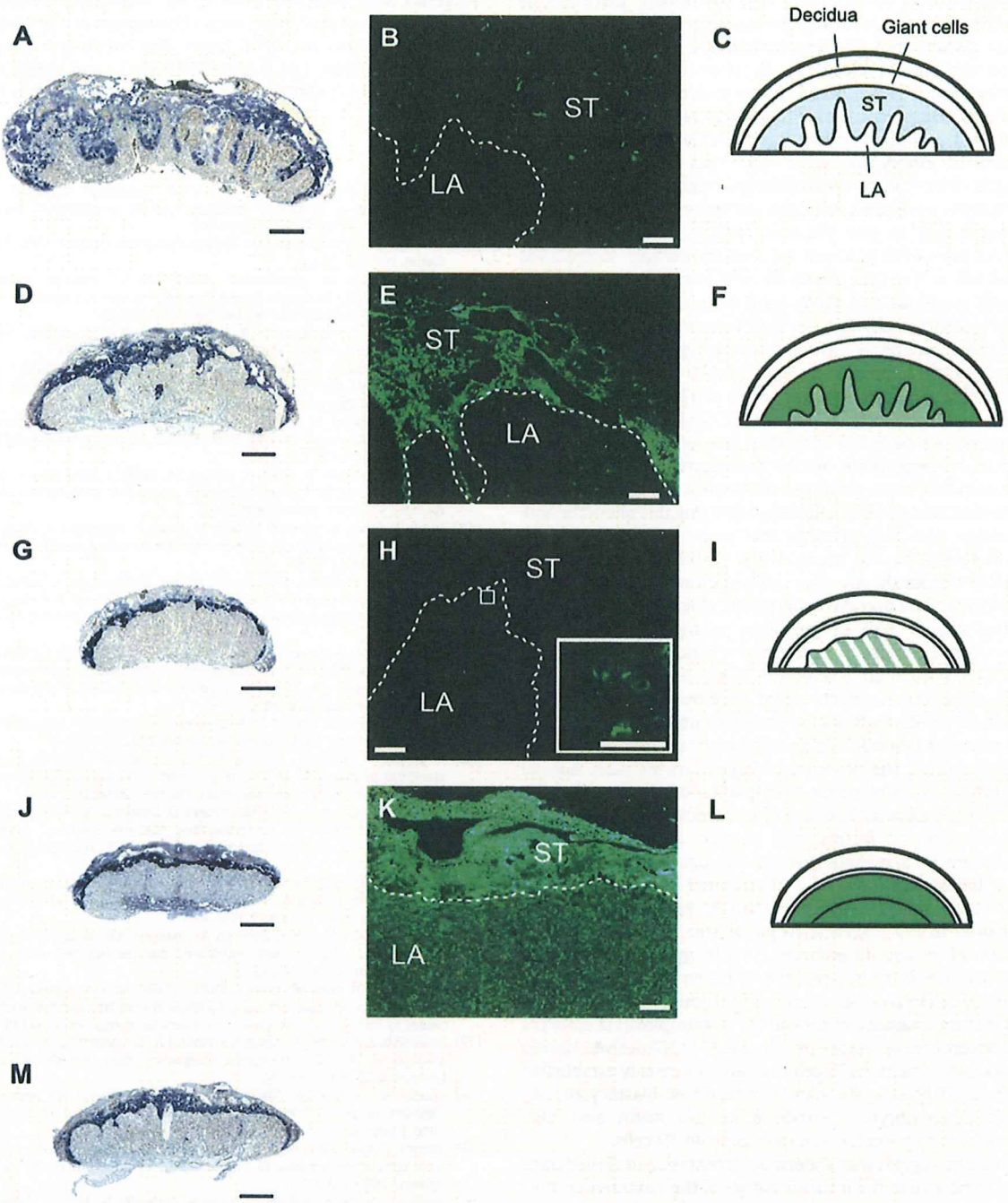

Fig. 1. Representative histology of placentas that developed from chimeric embryos, as shown by in situ hybridization for *Tpbpa* (a marker for the spongiotrophoblast layer; A, D, G), green fluorescent protein (GFP) fluorescence (B, E, H) and schematic illustrations (C, F, I). (A–C) 2*n* nuclear transfer (NT) derived ⇔ 4*n* fertilization-derived (FD) chimeric embryos. They show typical features of clone-specific hyperplastic placentas with a predominant contribution by non-GFP-expressing NT-derived cells. (D–F) 2*n* NT ⇔ 3 × 4*n* FD embryos also show hyperplastic placentation while the major components are of 4*n* FD origin expressing GFP. (G–I) 2*n* FD ⇔ 4*n* NT aggregations. The placental histology is nearly normal with only a slight enlargement, as that of 2*n* FD ⇔ 4*n* FD placentas (see M and Table 1), although non-GFP NT-derived cells predominate. The inset in H, a higher magnification of a small rectangle in the middle, indicates GFP-bearing fetal capillaries in the labyrinthine layer. (J–L) Control placentas from GFP-expressing 2*n* FD embryos as a reference for the normal morphology and the full intensity of GFP fluorescence in the labyrinthine and spongiotrophoblast layers. (M) A control placenta from a 2*n* FD ⇔ 4*n* FD embryo. It also shows normal-looking histology with only a slight enlargement. ST, spongiotrophoblast layer; LA, labyrinthine layer. Bars = 1 mm (A, D, G, and J), 200 μm (B, E, H, and K), and 50 μm (inset in H).

of the presence of non-GFP-expressing fetal capillaries in the labyrinthine layer (see Fig. 1H for the localization of the fetal capillaries). In their reciprocal combination, 2*n* FD ⇔ 4*n* NT, FD-derived cells were only found in the fetal capillaries in the labyrinthine layer and all other trophoblastic components were derived from NT cells (Fig. 1H).

Although the numbers of placentas analyzable were limited when the 2*n* embryos were the NT origin, we may outline typical

distribution patterns of 2*n* and 4*n* cells in chimeric placentas, as shown in Fig. 1C, F and I. These patterns suggest that the origin of embryonic tissues, not the extraembryonic tissues, had more impact on the size of placentas. In other words, hyperplastic placentation, which is attributed to excess proliferation of the ST layer cells, develops in a nonautonomous fashion. This is very intriguing, but a similar finding has recently been reported for aggregation of embryonic stem (ES) cells and 4*n* embryos. According to Ohta et al., chimeric embryos originating from ES cells and 4*n* embryos developed enlarged placentas [22]. While ES cells rarely contributed to the placental tissues, they consistently affected the size of the placenta even when multiple 4*n* embryos were used (up to 3×) [22]. As 4*n* NT cells also distributed to less hyperplastic placentas, the ploidy itself did not seem to affect the size of the placentas. Although our conclusions are drawn based on our repetitive experiments including several types of controls, they should be further confirmed by experiments using ES cells and trophoblast stem (TS) cells, both of which can be established from FD blastocysts as well as NT blastocysts [23,24].

At present, we have not identified the genetic or molecular factors that are responsible for the development of hyperplastic placentas in cloned mice. However, the present study may provide a clue to understand the mechanisms underlying this phenomenon. We and others have demonstrated that such hyperplastic placentation is preceded by the hypomorphic development of diploid trophoblastic tissues shortly after implantation [14,20]. Therefore, it is logical to assume that the hyperplastic placentation that arises during the second half of gestation is the consequence of a compensatory response to earlier perturbations. However, from our observations such an assumption might not be true because such early placentation defects might have been overcome when using multiple 4*n* FD embryos, as demonstrated by the increased numbers of implantation sites associated with large decidualization scars found at term. The presence of large scars indicates normal decidual formation in response to implantation signals from the embryos. Thus, hyperplastic placentation seems to be induced by some embryo-derived factors that become active from midgestation onward. Such presumptive factors might affect the ST layer directly, or indirectly through the labyrinthine layer.

We also found that NT cells rather than FD cells were distributed predominantly in the placental trophoblastic tissues despite the combination of 2*n* and 4*n* embryos. This is opposite to what we assumed, because 4*n* cells often overcome 2*n* cells in the extraembryonic tissues in 2*n* ⇔ 4*n* chimeras [25]. Jouneau et al. [14] also reported that the majority of diploid NT ⇔ tetraploid FD embryos had the extraembryonic ectoderm composed of NT-derived tissues at day 7 of development. As TS cell lines are more easily established in vitro from NT blastocysts than from fertilized blastocysts [24], NT-derived extraembryonic ectoderm in vivo might also have a high proliferation potential and overcome 4*n* FD cells.

These results suggest that abnormal placentation in cloned mice cannot be attributed to the intrinsic nature of their extraembryonic tissues but to some unknown factors derived from the embryonic side. As the mouse gene-targeting strategy has unraveled many factors responsible for embryonic–placental interactions [13,24], abnormal placentation in cloned mice may also provide a clue to understand the mechanisms regulating normal placentation, especially those of embryonic origin that might control the proliferation of trophoblastic lineage cells.

Acknowledgments

The GFP-expressing (green) mice (C57BL/6-Tg(CAG-EGFP)C14-Y01-FM131Osb) used in this study were originally generated by Professor M. Okabe (Osaka University) and were provided from the RIKEN Bioresource Center, with the support of the National Bio-Resources Project of MEXT, Japan. This work was supported by KAKENHI (20062012 [A.O.], 19300151 [A.O.] and 19880037 [H.M.]) and by a fund for RIKEN Super Postdoctoral Fellowship [H.M.].

References

[1] Yang X, Smith SL, Tian XC, Lewin HA, Renard JP, Wakayama T. Nuclear reprogramming of cloned embryos and its implications for therapeutic cloning. Nat Genet 2007;39:295–302.
[2] Wakayama T, Yanagimachi R. Cloning of male mice from adult tail-tip cells. Nat Genet 1999;22:127–8.
[3] Tanaka S, Oda M, Toyoshima Y, Wakayama T, Tanaka M, Yoshida N, et al. Placentomegaly in cloned mouse concepti caused by expansion of the spongiotrophoblast layer. Biol Reprod 2001;65:1813–21.
[4] Wakayama T, Yanagimachi R. Mouse cloning with nucleus donor cells of different age and type. Mol Reprod Dev 2001;58:376–83.
[5] Inoue K, Ogonuki N, Mochida K, Yamamoto Y, Takano K, Kohda T, et al. Effects of donor cell type and genotype on the efficiency of mouse somatic cell cloning. Biol Reprod 2003;69:1394–400.
[6] Inoue K, Wakao H, Ogonuki N, Miki H, Seino K, Nambu-Wakao R, et al. Generation of cloned mice by direct nuclear transfer from natural killer T cells. Curr Biol 2005;15:1114–8.
[7] Inoue K, Ogonuki N, Miki H, Hirose M, Noda S, Kim JM, et al. Inefficient reprogramming of the hematopoietic stem cell genome following nuclear transfer. J Cell Sci 2006;119:1985–91.
[8] Inoue K, Noda S, Ogonuki N, Miki H, Inoue S, Katayama K, et al. Differential developmental ability of embryos cloned from tissue-specific stem cells. Stem Cells 2007;25:1279–85.
[9] Shinmen A, Honda A, Ohkawa M, Hirose M, Ogonuki N, Yuzuriha M, et al. Efficient production of intersubspecific hybrid mice and embryonic stem cells by intracytoplasmic sperm injection. Mol Reprod Dev 2007;74:1081–8.
[10] Van Thuan N, Wakayama S, Kishigami S, Ohta H, Hikichi T, Mizutani E, et al. Injection of somatic cell cytoplasm into oocytes before intracytoplasmic sperm injection impairs full-term development and increases placental weight in mice. Biol Reprod 2006;74:865–73.
[11] Li Y, Behringer RR. Esx1 is an X-chromosome-imprinted regulator of placental development and fetal growth. Nat Genet 2001;20:309–11.
[12] Wakisaka N, Inoue K, Ogonuki N, Miki H, Sekita Y, Hanaki K, et al. Ultrastructure of placental hyperplasia in mice: comparison of placental phenotypes with three different etiologies. Placenta 2008;29:753–9.
[13] Sapin V, Blanchon L, Serre AF, Lemery D, Dastugue B, Ward SJ. Use of transgenic mice model for understanding the placentation: towards clinical applications in human obstetrical pathologies? Transgenic Res 2001;10:377–98.
[14] Jouneau A, Zhou Q, Camus A, Brochard V, Maulny L, Collignon J, et al. Developmental abnormalities of NT mouse embryos appear early after implantation. Development 2006;133:1597–607.
[15] Wakayama T, Perry ACF, Zuccotti M, Johnson KR, Yanagimachi R. Full-term development of mice from enucleated oocytes injected with cumulus cell nuclei. Nature 1998;394:369–74.
[16] Mochida K, Ohkawa M, Inoue K, Valdez Jr DM, Kasai M, Ogura A. Birth of mice after in vitro fertilization using C57BL/6 sperm transported within epididymides at refrigerated temperatures. Theriogenology 2005;64:135–43.
[17] Nakanishi T, Kuroiwa A, Yamada S, Isotani A, Yamashita A, Tairaka A, et al. FISH analysis of 142 EGFP transgene integration sites into the mouse genome. Genomics 2002;80:564–74.
[18] Chatot CL, Ziomek CA, Bavister BD, Lewis JL, Torres I. An improved culture medium supports development of random-bred 1-cell mouse embryos in vitro. J Reprod Fertil 1989;86:679–88.
[19] Nagy A, Gocza E, Diaz EM, Prideaux VR, Ivanyi E, Markkula M, et al. Embryonic stem cells alone are able to support fetal development in the mouse. Development 1990;110:815–21.
[20] Wakisaka Saito N, Kohda T, Inoue K, Ogonuki N, Miki H, Hikichi T, et al. Chorioallantoic placenta defects in cloned mice. Biochem Biophys Res Commun 2006;349:106–14.
[21] Li J, Ishii T, Wen D, Mombaerts P. Non-equivalence of cloned and clonal mice. Curr Biol 2005;15:R756–7.
[22] Ohta H, Sakaide Y, Yamagata K, Wakayama T. Increasing the cell number of host tetraploid embryos can improve the production of mice derived from embryonic stem cells. Biol Reprod 2008;79:486–92.
[23] Wakayama T. Production of cloned mice and ES cells from adult somatic cells by nuclear transfer: how to improve cloning efficiency? J Reprod Dev 2007;53:13–26.
[24] Rielland M, Hue I, Renard JP, Alice J. Trophoblast stem cell derivation, cross-species comparison and use of nuclear transfer: new tools to study trophoblast growth and differentiation. Dev Biol 2008;322:1–10.
[25] MacKay GE, West JD. Fate of tetraploid cells in 4*n* <–> 42*n* chimeric mouse blastocysts. Mech Dev 2005;122:1266–81.

LETTER

Changes in Allele-Specific Association of Histone Modifications at the Imprinting Control Regions During Mouse Preimplantation Development

Jin-Moon Kim and Atsuo Ogura*
RIKEN Bioresource Center, Tsukuba, Ibaraki, Japan

Received 13 February 2009; Revised 8 May 2009; Accepted 14 May 2009

Summary: Allele-specific association of histone modification is observed at the regulatory region of imprinted genes and has been suggested to work as an epigenetic marker for monoallelic gene expression, along with the allelic CpG methylation of DNA. Although the parent-origin-specific epigenetic status in imprinted genes is thought to be established during preimplantation development, little is known about the allelic specificity of histone modifications during this period because of the limited volume of material available for analysis. In this study, we first revealed the allelic enrichment of histone modifications and variant histones at the imprinting control regions (ICRs) of four-cell to blastocyst stage preimplantation embryos by using carrier chromatin immunoprecipitation and sequence polymorphism analysis of immunoprecipitated DNA. We found relative enrichment of histone H3 lysine 9 dimethylation at the imprinted alleles of ICRs and obtained the results suggesting that histone modifications at ICRs are established during a late preimplantation stage. genesis 47:611–616, 2009. © 2009 Wiley-Liss, Inc.

Key words: histone modification; variant histone; genomic imprinting; preimplantation development; mouse

The sex-specific epigenetic modifications that are imposed during gametogenesis act as a primary imprinting memory to distinguish maternal and paternal alleles and direct specific expression of imprinted genes. The imprinted genes are characterized by CpG dinucleotide-rich regions called differentially methylated regions (DMRs), for which DNA methylation levels differ between the maternal and paternal alleles (Reik and Walter, 2001). Some of these DMRs function as imprinting control regions (ICRs) and impose epigenetic influences on neighboring imprinted genes (Edwards and Ferguson-Smith, 2007). Gene knockout studies showed that deletions of these ICRs result in disturbance of allele-specific expression of the imprinted genes (Fitzpatrick *et al.*, 2002; Lin *et al.*, 2003). It has also been reported that differential histone modifications on the ICRs-repressive histone modifications for imprinted ICRs while active histone modifications for another alleles, are involved in the regulation of imprinted genes in *cis* (Fournier *et al.*, 2002). In fact, embryonic stem cells lacking histone H3 lysine 9 (H3K9) methyltransferase G9a show loss of imprinting in *Snrpn* (Xin *et al.*, 2003) and mice lacking G9a lost their imprinted repression of placenta-specific imprinted genes (Wagschal *et al.*, 2008). These observations highlight the involvement of histone modifications in the maintenance of genomic imprinting memory.

An increase in the frequency of imprinting disorders such as Angelman syndrome (Cox *et al.*, 2002) and Beckwith-Wiedermann syndrome (DeBaun *et al.*, 2003) in the children conceived by assisted reproduction technology (ART) demonstrates the importance of understanding the profiles of epigenetic marks that are involved in imprinting memory as early as possible in embryogenesis, because the imprinting status is fixed at fertilization. Allele-specific DNA methylation of ICRs in preimplantation embryos has been reported (Yatsuki *et al.*, 2002) and is known to be regulated by DNA (cytosine-5-)-methyltransferase 1 (Dnmt1) (Hirasawa *et al.*, 2008). However, little is known about the allelic specificities of histone modifications during preimplantation development because conventional chromatin immunoprecipitation (ChIP) experiments ideally require five million cells or more, and such a number is hard to achieve with preimplantation embryos. In this study, we developed a method that enabled us to examine the relative enrichment of histone modifications in each parental allele of the ICRs in mouse preimplantation embryos, by modifying a carrier chromatin immunoprecipitation (CChIP) technique originally developed for epigenetic characterization of small cell populations (O'Neill *et al.*, 2006).

In our preliminary study, we performed a single strand conformation polymorphism (SSCP) analysis of currently reported ICRs. We found that polymerase chain reaction (PCR) products amplifying the KvDMR1 alleles of Chromosome 7, and IG-DMR alleles of Chromosome 12, are easily distinguishable between C57BL/6 (B6) mice and

*Correspondence to: Atsuo Ogura, RIKEN Bioresource Center, Tsukuba, Ibaraki, Japan. E-mail: ogura@rtc.riken.jp
Contract grant sponsors: MEXT, JSPS
Published online 15 June 2009 in
Wiley InterScience (www.interscience.wiley.com).
DOI: 10.1002/dvg.20541

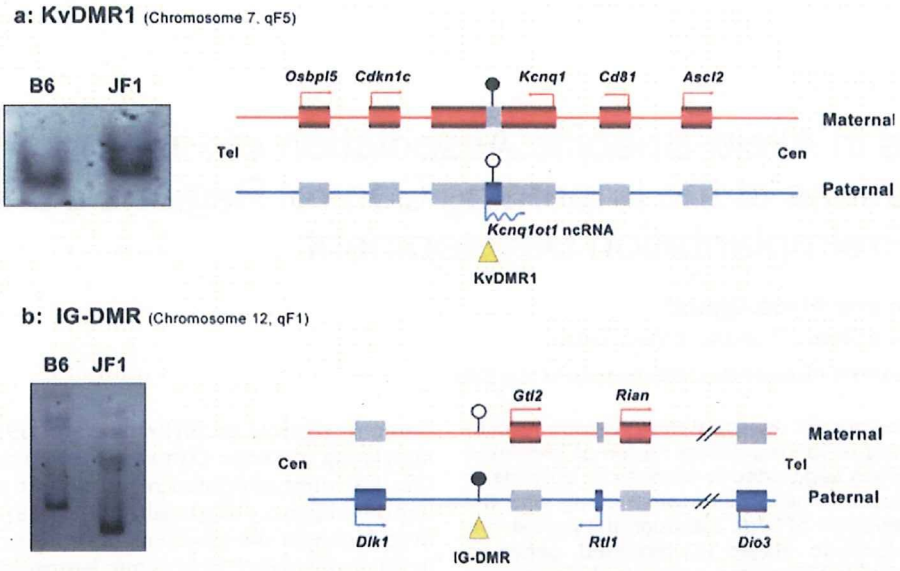

FIG. 1. Distinguishing the parental origin of the KvDMR1 allele (**a**) and IG-DMR allele (**b**) between C57BL/6 and JF1 mouse strain genomes using single strand conformation polymorphism (SSCP) or simple sequence length polymorphism (SSLP) analyses, respectively. Black and white lollipops indicate germline DNA methylation and DNA unmethylation, respectively. Yellow arrowheads indicate the positions of imprinting control regions (ICRs).

JF1 mice using polyacrylamide gel electrophoresis (Fig. 1a,b). KvDMR1, also known as IC2, is a CpG island in *Kcnq1* that is methylated during oocyte maturation (Hiura *et al.*, 2006) and contains the promoter for a paternally expressed noncoding RNA (ncRNA) *Kcnq1ot1*, which is involved in paternal repression along the *kcnq1* domain (Fitzpatrick *et al.*, 2002; Mancini-DiNardo *et al.*, 2003). Maternal and paternal allele of KvDMR1 is associated with repressive and active histone marks, respectively (Umlauf *et al.*, 2004). The IG-DMR, located between *Dlk1* and *Gtl2* (Takada *et al.*, 2002), is specifically methylated in the male germline (Li *et al.*, 2004) and regulates the parental allele-specific expression of neighboring imprinted genes (Lin *et al.*, 2003). It has been reported that allele-specific histone acetylation regulates expression of the *Dkl1-Gtl2* imprinted domain (Carr *et al.*, 2007). Here we describe the allele-specific histone modification profiles of these two ICRs during mouse preimplantation embryo development.

First, we investigated allelic differences in histone modifications at KvDMR1. After collecting four-cell, morula and blastocyst stage preimplantation embryos prepared by the fertilization of B6 strain oocytes with JF1 spermatozoa, we carried out CChIP with antibodies against transcriptionally repressive histone modifications such as histone H3K9 dimethylation (H3K9me2), H3K27 trimethylation (H3K27me3), and transcriptionally active histone modifications such as H4K12 acetylation (H4K12ac). Additionally, histone variant macroH2A1 (mH2A1) antibody was used because macroH2A1 associates preferentially with the inactive X chromosome (Costanzi and Pehrson, 1998) and with imprinted ICRs (Choo *et al.*, 2006). Parental enrichment of immunoprecipitated alleles were analyzed using PCR-SSCP, as described in Figure 1a. From the four-cell to blastocyst stages, the repressive H3K9me2 mark showed maternal enrichment while H4K12ac, an active histone mark, was enriched in the paternal allele at the morula to the blastocyst stage (Fig. 2a–c). H3K27me3 showed maternal enrichment from the four-cell to the morula stage but there was no maternal bias at the blastocyst stage. These results suggest that these repressive histone marks, especially H3K9me2, work as epigenetic markers of imprinted KvDMR1 before implantation. The absence of bias for H3K27me3 at the blastocyst stage is consistent with results obtained from embryonic stem cells and trophoblast stem cells (Lewis *et al.*, 2006).

Next, we investigated allelic enrichment of histone modifications at IG-DMR, which is methylated during spermatogenesis (Li *et al.*, 2004). Because the PCR product obtained from JF1 is 18 bp shorter than the B6 amplicon, it is easy to discriminate the parental origin of the immunoprecipitated IG-DMR allele from B6 × JF1 hybrid embryos, as described in Figure 1b. Interestingly, the association of H3K9me2 with the paternal IG-DMR allele was found only after the morula stage and paternally biased H3K27me3 was shown at the blastocyst stage. At the four-cell stage, neither paternal nor maternal enrichment of repressive histone modifications were observed (Fig. 3a–c).

The developmental changes in maternal-to-paternal and paternal-to-maternal enrichment ratios of each histone modification and variant histone are summarized in right column in Figures 2 and 3. This compares the chro-

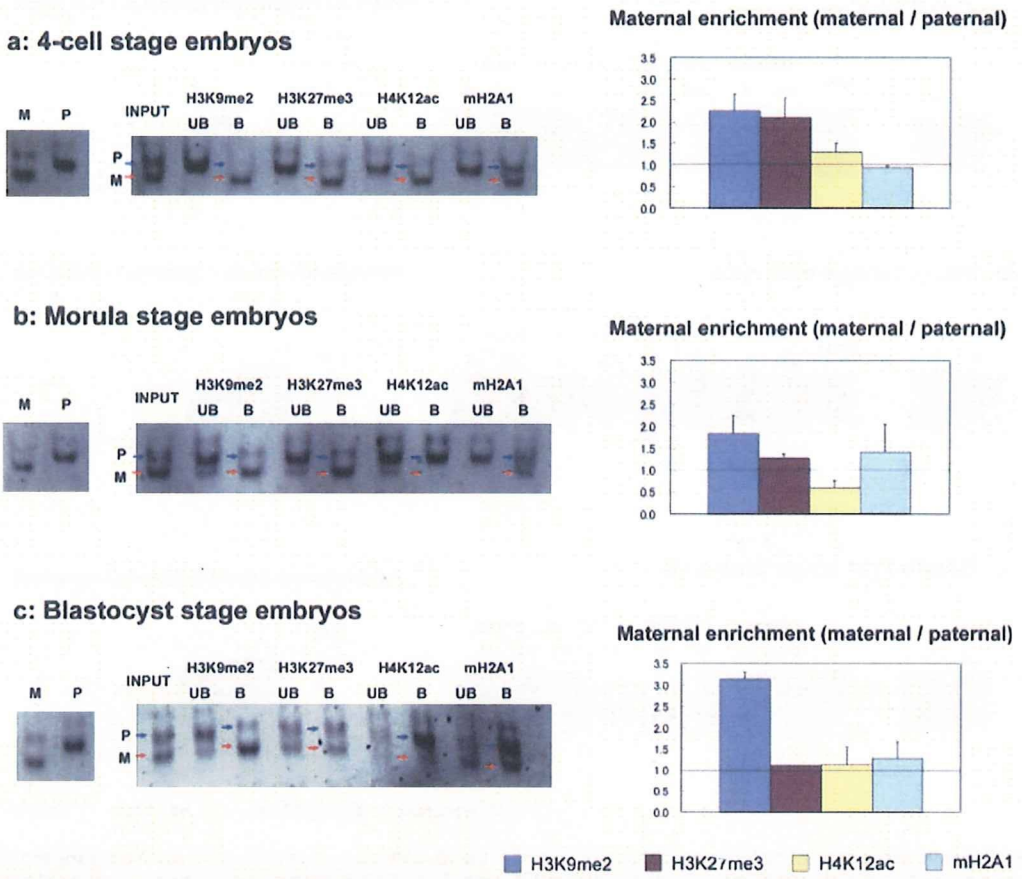

FIG. 2. Allele-specific association of a histone modification or variant histone at the KvDMR1 sequence of four-cell (**a**), morula (**b**) and blastocyst (**c**) stage embryos obtained from in vitro fertilization between B6 and JF1 strain mice. Allelic carrier chromatin immunoprecipitation (CChIP) assays were carried out using antibodies directed against H3K9me2, H3K27me3, H4K12ac, and macroH2A1. CChIP material was amplified by PCR and parental alleles of KvDMR1 were distinguished by SSCP. Results are representative of two independent CChIP experiments. The right panels represent the degree of maternal enrichment calculated by dividing the maternal band value with the paternal one (normalized according to the input). Error bars represent the standard error of the mean calculated from three PCR-SSCP gel repeat experiments. Key: P, paternal; M, maternal; UB, unbound fraction; B, bound fraction.

matin modification profile of KvDMR1 and IG-DMR. KvDMR1 showed significant maternal association of H3K9me2 throughout preimplantation development while paternal association of IG-DMR appeared after the morula stage. These differences in H3K9 methylation pattern profile might be attributable to the protamine-histone exchanges that occur in the male pronucleus after fertilization (Nonchev and Tsanev, 1990) and subsequent H3K9me2 asymmetry between the paternal and maternal genomes (Liu *et al.*, 2004). The results that all histone modifications investigated at KvDMR1 were maternally enriched at the four-cell stage implies that epigenetic asymmetry between the maternal and paternal genomes persists to the four-cell stage. The lack of paternal H3K9me2 enrichment of IG-DMR at the four-cell stage suggests that the imprinting memory originated from the paternal germline is maintained mainly by allelic DNA methylation until this stage.

After fertilization, gene expression in differentiated gametes is reprogrammed to allow the initiation of a new program from the totipotent zygotic genome. In spite of these remarkable transformations in gene expression profiles, the imprinting memory that discriminates paternal and maternal genomes must be maintained because the parental genomes are functionally distinct. Although it has been known that ICRs remain highly methylated despite global DNA-hypomethylation during preimplantation development (Yatsuki *et al.*, 2002), it is still unclear why ICRs are resistant to genome-wide demethylation. The observation that H3K9me2 associates with imprinted ICRs regardless of its germline origin suggests that it is involved in protecting ICRs from hypomethylation during early development. Hirasawa *et al.* (2008) reported that Dnmt1 maintains the DNA methylation of DMRs during preimplantation development. Considering that H3K9me2

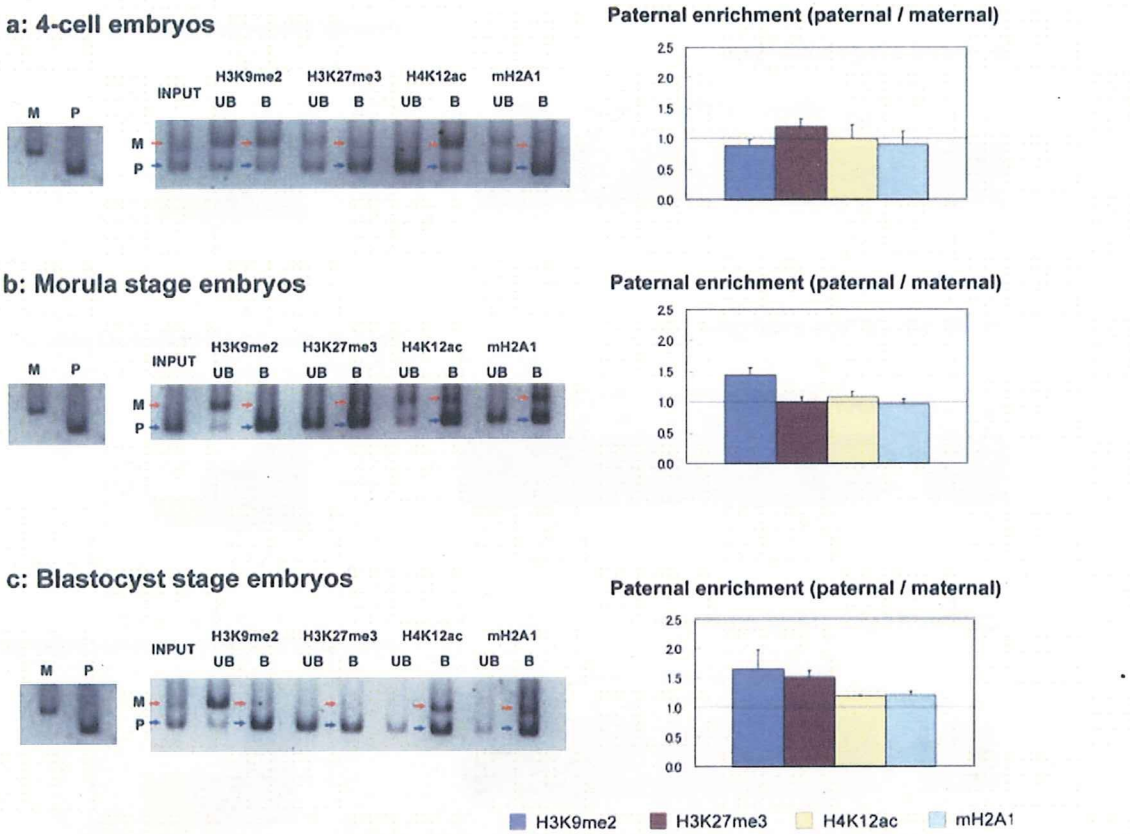

FIG. 3. Allele-specific association of histone modification or variant in the IG-DMR sequence of four-cell (**a**), morula (**b**) and blastocyst (**c**) stage embryos obtained from in vitro fertilization between B6 and JF1 mice. Allelic CChIP assays were carried out using antibodies directed against H3K9me2, H3K27me3, H4K12ac, and macroH2A1. CChIP material was amplified by PCR and parental alleles of the IG-DMR sequence were distinguished by SSLP analysis. Results are representative of two independent CChIP experiments. The right panels represent the degree of paternal enrichment calculated by dividing the paternal band value with the maternal one (normalized according to the input). Error bars represent the standard error of the mean calculated from three PCR-SSLP gel repeat experiments. Key: P, paternal; M, maternal; UB, unbound fraction; B, bound fraction.

provides a binding platform for heterochromatin protein 1 (HP1) (Lachner *et al.*, 2001) and there is a functional link between HP1 and Dnmt1 (Smallwood *et al.*, 2007), it is plausible that H3K9me2 reinforces imprinting memory by facilitating the interconnection of HP1 and Dnmt1 during preimplantation development.

Unlike previous reports of preferential deposition towards inactive methylated ICR alleles in brain and liver tissue (Choo *et al.*, 2006) and specific accumulation to the inactive X chromosome in extraembryonic lineages of blastocysts (Costanzi *et al.*, 2000), we could not detect significant allelic enrichment of macroH2A1 in ICRs of preimplantation mouse embryos. This discordance in the allelic association pattern of macro H2A1 and the low genomic incorporation of macroH2A until the eight-cell stage in mouse embryos (Chang *et al.*, 2005) together imply that specific localization of macroH2A1 is not established in the early stage of development.

To our knowledge, this is the first demonstration of the allelic differences in histone modifications and variant histone deposition of ICRs in mammalian preimplantation embryos. The knowledge obtained from this study will contribute to elucidating the epigenetic mechanisms underlying genomic reprogramming and the maintenance of imprinting memory after fertilization.

METHODS

Preparation of Embryos

Female C57BL/6 strain female mice (SLC, Shizuoka, Japan), 8 weeks of age, were superovulated with 5 IU of pregnant mare serum gonadotrophin, followed 48 h later with 5 IU of human chorionic gonadotrophin (hCG). Unfertilized metaphase II-stage arrested oocytes were collected in human tubal fluid (HTF) medium from the ampullae of oviducts, 14–15 h after hCG injection.

Sperm were collected from the caudal epididymis of adult Japanese fancy 1 (JF1) strain male mice and preincubated in HTF for 2 h in an atmosphere of 5% CO_2, 95% air at 37.5°C. The oocytes were inseminated with capacitated sperm. Three hours after insemination, the fertilized oocytes were washed and cultured in KSOM (Lawitts and Biggers, 1993). Morula and blastocyst stage embryos were collected at 72 and 96 h after insemination, respectively.

ChIP

CChIP experiments were carried out in the presence of *Drosophila* S2 cells with slight modifications of a protocol reported by O'Neill *et al.* (2006). For each CChIP experiment, 9×10^7 S2 cells were used as carrier cells for the ChIP of preimplantation embryos. We used 110–200 preimplantation embryos in each CChIP experiment. After purification of nuclei collected by ultracentrifuge through a sucrose cushion, 30 U of micrococcal nuclease (Takara Bio, Shiga, Japan) was added and incubated for 6 min at 37°C. Approximately, 30 μg of unfixed chromatin was incubated with 5 μg of antibody overnight at 4°C. We used the following antibodies: H3K9 dimethylation (Abcam, Cambridge, MA; ab1220), H3K27 trimethylation (Abcam; ab6002), acetylated H4K12 (Upstate, 06-761), macroH2A1 (Upstate, 07-219). The antibody chromatin complexes were captured by 4-h incubation with Protein-A Sepharose beads. Bound fraction chromatin was obtained after washing with 0.1–0.2 M NaCl and elution with 1% SDS. DNA was extracted from the input chromatin, bound and unbound fractions by phenol-chloroform extraction followed by ethanol precipitation.

SSCP and SSLP Analysis for Distinguishing the C57BL/6 and JF1 Alleles

Allele-specific association of histone modifications was analyzed for paternal and maternal alleles using SSCP or simple sequence length polymorphism (SSLP) to distinguish between *Mus musculus domesticus* (C57BL/6) and *Mus musculus molossinus* (JF1) genomes. The primer sequences for IG-DMR and KvDMR1 amplification were adopted from Delaval *et al.* (2007). KvDMR1 was amplified 40 cycles under the following conditions with forward primer 5′-ACTTCCGTGTGGATCGTTTC-3′ and reverse primer 5′-GAGAACCATGCCGAGAAAAA-3′: 94°C for 30 s, 55°C for 30 s, and 72°C for 30 s. IG-DMR was amplified using 40 cycles under the following conditions with forward primer 5′-GGAAGACAAAGAGCAA GCCTGT-3′ and reverse primer 5′-CTAGACCAACGGTG AGCCAGGAT-3′: 94°C for 30 s, 55°C for 30 s, and 72°C for 30 s. The PCR products were separated on 6% polyacrylamide gels, with 5% glycerol for KvDMR1, and without for IG-DMR. Gels were stained with SYBR gold (Molecular Probes, Eugene, OR) for KvDMR1 and SYBR green I (Invitrogen, Carlsbad, CA) for IG-DMR. The fluorescence was detected using a LAS-1000 image analyzer (Fujifilm, Tokyo, Japan) and band patterns were quantified using Scion Image for Windows software (National Institutes of Health, Bethesda, MD).

ACKNOWLEDGMENTS

The JF1 strain (*M. m. molossinus*) used in this study was provided by RIKEN Bioresource Center, with the support of the National BioResources Project of MEXT, Japan.

LITERATURE CITED

Carr MS, Yevtodiyenko A, Schmidt CL, Schmidt JV. 2007. Allele-specific histone modifications regulate expression of the Dlk1-Gtl2 imprinted domain. Genomics 89:280–290.

Chang CC, Ma Y, Jacobs S, Tian XC, Yang X, Rasmussen TP. 2005. A maternal store of macroH2A is removed from pronuclei prior to onset of somatic macroH2A expression in preimplantation embryos. Dev Biol 278:367–380.

Choo JH, Kim JD, Chung JH, Stubbs L, Kim J. 2006. Allele-specific deposition of macroH2A1 in imprinting control regions. Hum Mol Genet 15:717–724.

Costanzi C, Pehrson JR. 1998. Histone macroH2A1 is concentrated in the inactive X chromosome of female mammals. Nature 393:599–601.

Costanzi C, Stein P, Worrad DM, Schultz RM, Pehrson JR. 2000. Histone macroH2A1 is concentrated in the inactive X chromosome of female preimplantation mouse embryos. Development 127:2283–2289.

Cox GF, Burger J, Lip V, Mau UA, Sperling K, Wu BL, Horsthemke B. 2002. Intracytoplasmic sperm injection may increase the risk of imprinting defects. Am J Hum Genet 71:162–164.

DeBaun MR, Niemitz EL, Feinberg AP. 2003. Association of in vitro fertilization with Beckwith-Wiedemann syndrome and epigenetic alterations of LIT1 and H19. Am J Hum Genet 72:156–160.

Delaval K, Govin J, Cerqueira F, Rousseaux S, Khochbin S, Feil R. 2007. Differential histone modifications mark mouse imprinting control regions during spermatogenesis. EMBO J 26:720–729.

Edwards CA, Ferguson-Smith AC. 2007. Mechanisms regulating imprinted genes in clusters. Curr Opin Cell Biol 19:281–289.

Fitzpatrick GV, Soloway PD, Higgins MJ. 2002. Regional loss of imprinting and growth deficiency in mice with a targeted deletion of KvDMR1. Nat Genet 32:426–431.

Fournier C, Goto Y, Ballestar E, Delaval K, Hever AM, Esteller M, Feil R. 2002. Allele-specific histone lysine methylation marks regulatory regions at imprinted mouse genes. EMBO J 21:6560–6570.

Hirasawa R, Chiba H, Kaneda M, Tajima S, Li E, Jaenisch R, Sasaki H. 2008. Maternal and zygotic Dnmt1 are necessary and sufficient for the maintenance of DNA methylation imprints during preimplantation development. Genes Dev 22:1607–1616.

Hiura H, Obata Y, Komiyama J, Shirai M, Kono T. 2006. Oocyte growth-dependent progression of maternal imprinting in mice. Genes Cells 11:353–361.

Lachner M, O'Carroll D, Rea S, Mechtler K, Jenuwein T. 2001. Methylation of histone H3 lysine 9 creates a binding site for HP1 proteins. Nature 410:116–120.

Lawitts JA, Biggers JD. 1993. Culture of preimplantation embryos. Methods Enzymol 225:153–164.

Lewis A, Green K, Dawson C, Redrup L, Huynh KD, Lee JT, Hemberger M, Reik W. 2006. Epigenetic dynamics of the Kcnq1 imprinted domain in the early embryo. Development 133:4203–4210.

Li JY, Lees-Murdock DJ, Xu GL, Walsh CP. 2004. Timing of establishment of paternal methylation imprints in the mouse. Genomics 84:952–960.

Lin SP, Youngson N, Takada S, Seitz H, Reik W, Paulsen M, Cavaille J, Ferguson-Smith AC. 2003. Asymmetric regulation of imprinting on the maternal and paternal chromosomes at the Dlk1-Gtl2 imprinted cluster on mouse chromosome 12. Nat Genet 35:97–102.

Liu H, Kim JM, Aoki F, Ogura A, Nagata M. 2004. Regulation of histone H3 lysine 9 methylation in oocytes and early pre-implantation embryos. Development 131:2269–2280.

Mancini-DiNardo D, Steele SJ, Ingram RS, Tilghman SM. 2003. A differentially methylated region within the gene Kcnq1 functions as an imprinted promoter and silencer. Hum Mol Genet 12:283–294.

Nonchev S, Tsanev R. 1990. Protamine-histone replacement and DNA replication in the male mouse pronucleus. Mol Reprod Dev 25:72–76.

O'Neill LP, VerMilyea MD, Turner BM. 2006. Epigenetic characterization of the early embryo with a chromatin immunoprecipitation protocol applicable to small cell populations. Nat Genet 38:835–841.

Reik W, Walter J. 2001. Genomic imprinting: Parental influence on the genome. Nat Rev Genet 2:21–32.

Smallwood A, Esteve PO, Pradhan S, Carey M. 2007. Functional cooperation between HP1 and DNMT1 mediates gene silencing. Genes Dev 21:1169–1178.

Takada S, Paulsen M, Tevendale M, Tsai CE, Kelsey G, Cattanach BM, Ferguson-Smith AC. 2002. Epigenetic analysis of the Dlk1-Gtl2 imprinted domain on mouse chromosome 12: Implications for imprinting control from comparison with Igf2-H19. Hum Mol Genet 11:77–86.

Umlauf D, Goto Y, Cao R, Cerqueira F, Wagschal A, Zhang Y, Feil R. 2004. Imprinting along the Kcnq1 domain on mouse chromosome 7 involves repressive histone methylation and recruitment of Polycomb group complexes. Nat Genet 36:1296–1300.

Wagschal A, Sutherland HG, Woodfine K, Henckel A, Chebli K, Schulz R, Oakey RJ, Bickmore WA, Feil R. 2008. G9a histone methyltransferase contributes to imprinting in the mouse placenta. Mol Cell Biol 28:1104–1113.

Xin Z, Tachibana M, Guggiari M, Heard E, Shinkai Y, Wagstaff J. 2003. Role of histone methyltransferase G9a in CpG methylation of the Prader-Willi syndrome imprinting center. J Biol Chem 278:14996–15000.

Yatsuki H, Joh K, Higashimoto K, Soejima H, Arai Y, Wang Y, Hatada I, Obata Y, Morisaki H, Zhang Z, Nakagawachi T, Satoh Y, Mukai T. 2002. Domain regulation of imprinting cluster in Kip2/Lit1 subdomain on mouse chromosome 7F4/F5: Large-scale DNA methylation analysis reveals that DMR-Lit1 is a putative imprinting control region. Genome Res 12:1860–1870.

Journal of Reproduction and Development, Vol. 55, No. 5, 2009

—Full Paper—

Sex-Reversed Somatic Cell Cloning in the Mouse

Kimiko INOUE[1,2], Narumi OGONUKI[1], Kazuyuki MEKADA[1], Atsushi YOSHIKI[1], Takashi SADO[3] and Atsuo OGURA[1,2,4]

[1]BioResource Center, RIKEN, Ibaraki 305-0074, [2]Graduate School of Life and Environmental Sciences, University of Tsukuba, Ibaraki 305-8571, [3]Department of Molecular Genetics, Medical Institute of Bioregulation, Kyushu University, Fukuoka 812-8582 and [4]The Center for Disease Biology and Integrative Medicine, Faculty of Medicine, University of Tokyo, Tokyo 113-0033, Japan

Abstract. Somatic cell nuclear transfer has many potential applications in the fields of basic and applied sciences. However, it has a disadvantage that can never be overcome technically—the inflexibility of the sex of the offspring. Here, we report an accidental birth of a female mouse following nuclear transfer using an immature Sertoli cell. We produced a batch of 27 clones in a nuclear transfer experiment using Sertoli cells collected from neonatal male mice. Among them, one pup was female. This "male-derived female" clone grew into a normal adult and produced offspring by natural mating with a littermate. Chromosomal analysis revealed that the female clone had a 39,X karyotype, indicating that the Y chromosome had been deleted in the donor cell or at some early step during nuclear transfer. This finding suggests the possibility of resuming sexual reproduction after a single male is cloned, which should be especially useful for reviving extinct or endangered species.

Key words: Mouse, Nuclear transfer, Sertoli cell, Sex reversal

(J. Reprod. Dev. 55: 566–569, 2009)

Although somatic cell nuclear transfer (SCNT) has been successfully applied as a reproductive technique without gametes to a wide range of mammalian species, the rates of full-term development are still very low, irrespective of the species or the donor cell type used [1]. However, many researchers are intensively studying the epigenetics of genomic reprogramming, and indeed, some significant improvements have recently been achieved [2, 3]. In the near future, the low efficiency of SCNT should not be an insuperable problem [1]. In contrast, another problem associated with SCNT that seems very difficult to overcome is the inflexibility of the sex of the offspring. Cloning male cells inevitably results in the birth of males, not females, and vice versa. This sex irreversibility may become an important issue, especially when sexual breeding must be resumed for subsequent propagation, e.g., in projects for resurrection of extinct species or rescue of endangered species. Recently, two Japanese groups have reported the birth of normal clones following nuclear transfer cloning with somatic cells retrieved from bodies or organs frozen for many years [4, 5]. These studies are encouraging to those who want to bring back the woolly mammoths lying frozen under the Siberian permafrost. In such cases, all the anticipated clones would be the same sex as the donor, and they would never propagate by natural breeding.

In a recent cloning experiment, we obtained a female mouse from an immature Sertoli cell. This "male-derived female" clone grew into a normal adult and produced offspring by natural mating. Although this was an accidental phenomenon arising from a sex-chromosomal error, the result unequivocally suggests the possibility of producing females from male donor animals if the techniques of sex chromosome manipulation are sufficiently well developed. Here, we report a case of sex-reversed SCNT in the mouse.

Accepted for publication: June 9, 2009
Published online in J-STAGE: July 14, 2009
Correspondence: A Ogura (e-mail: ogura@rtc.riken.jp) and K Inoue (e-mail: inoue@rtc.riken.jp)

Materials and Methods

Animals

The nuclear donor strain, (B6x129)F1, was obtained by mating two strains, an $Xist^{1loxGFP}$ C57BL/6 female (BioResource Center [BRC] no. RBRC01260) and a 129/Sv-*ter* male (CLEA Japan, Tokyo, Japan). The $Xist^{1loxGFP}$ C57BL/6 line was originally generated by Sado *et al.* [6]. In our laboratory, these knockout mice have been used to examine the effects of *Xist* downregulation on the development of clones, and we believe that such genetic modification had no relation to the finding in this report. Eight- to 10-week-old (C57BL/6 × DBA/2)F1 (BDF1, Japan SLC, Shizuoka, Japan) and 8–12-week-old ICR (CLEA Japan) female mice were used for the collection of the recipient oocytes and as embryo transfer recipients, respectively. The mice were maintained under specific-pathogen-free conditions. They were provided with water and commercial laboratory mouse chow *ad libitum* and housed under controlled lighting conditions (daily light period of 0700–2100 h). All animals were maintained in accordance with the guidelines of the RIKEN BioResource Center.

Preparation of donor cells

Immature Sertoli cells were collected from day 7 male neonates. The cells were prepared as described previously [7]. Briefly, the collected testicular cells were treated with 0.1 mg/mL collagenase (Sigma Chemical, St Louis, MO, USA) and 0.01 mg/ml deoxyribonuclease (Sigma) for 30 min at 37 C followed by 0.2 mg/ml trypsin (Sigma) for 5 min at 37 C. The testicular cell suspension was washed with Ca^{2+}/Mg^{2+}-free phosphate-buffered saline (PBS) con-

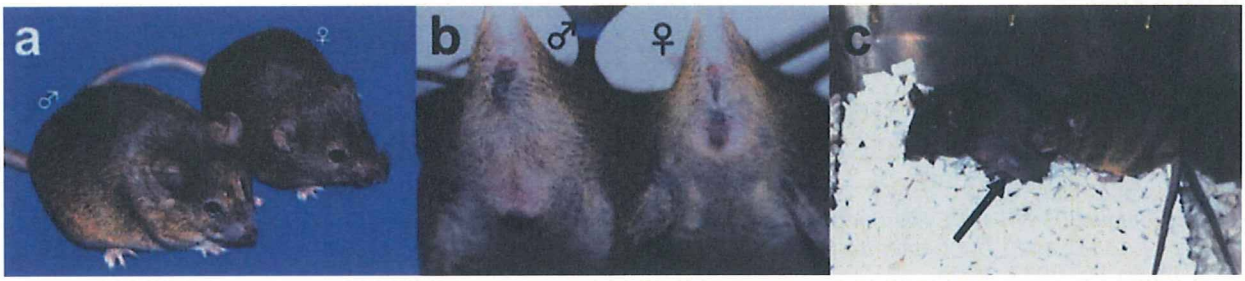

Fig. 1. a, b) Gross appearance (a) and external genitalia (b) of a female mouse and a male mouse cloned from Sertoli cells. c) Offspring (arrow) born from the female cloned mouse. The fertility of the female clone was confirmed by pregnancy and birth of normal offspring.

taining 4 mg/ml bovine serum albumin and used for injection.

Nuclear transfer

Nuclear transfer was carried out as described previously, with slight modifications [2, 7, 8]. The BDF1 female mice were induced to superovulate by the injection of 7.5 IU of pregnant mare serum gonadotropin (Sankyo Yell, Tokyo, Japan) and 7.5 IU of human chorionic gonadotropin (hCG; Aska Pharmaceutical, Tokyo, Japan) with a 48-h interval between the injections. At 15 h after the hCG injection, cumulus-oocyte complexes were collected from the oviducts, and the cumulus cells were dispersed in KSOM medium containing 0.1% bovine testicular hyaluronidase (Calbiochem, San Diego, CA, USA). The oocytes were enucleated in Hepes-buffered KSOM containing 7.5 μg/ml cytochalasin B. The donor nuclei were injected into enucleated oocytes with a Piezo-driven micromanipulator. After culture in KSOM for 1 h, the injected oocytes were activated in Ca^{2+}-free KSOM containing 2.5 mM $SrCl_2$ and 5 nM trichostatin A (TSA; Sigma) for 1 h. The reconstructed embryos were cultured in KSOM containing 5 μg/ml cytochalasin B and 5 nM TSA for 5 h, and then in KSOM containing 5 nM TSA for 2 h.

Embryo transfer

The reconstructed embryos that had reached the four-cell stage after 48 h in culture were transferred into the oviducts of pseudopregnant ICR female mice on day 0.5 (the day following sterile mating). On day 19.5, the pregnant females underwent Caesarian section, and the live pups were nursed by lactating ICR females.

Chromosomal analysis

Tail-tip fibroblasts were subjected to chromosomal analysis. The fibroblast cells were treated with 25 ng/ml colcemide for 4–6 h in culture dishes. The cells were collected by trypsinization, treated with 0.075 M KCl for 15 min at 37 C, and fixed with methanol:acetic acid (3:1). The cell suspensions were spread onto clean glass slides and allowed to dry in air. The prepared slides were stained with 5% Giemsa solution (Merck, Darmstadt, Germany) and examined with a light microscope using a 100× objective lens (Nikon, Tokyo, Japan). For Q-banding staining, the cells were stained by a combined quinacrine-33258 Hoechst method [9]. Metaphase images were observed under a fluorescent microscope, and karyotype analysis was performed using an Ikaros karyotyping system (Carl Zeiss, Jena, Germany).

Results and Discussion

We reconstructed 347 embryos by nuclear transfer using immature Sertoli cells. After 48 h in culture, 196 embryos (56.5%) had developed to the four-cell stage and were transferred into the oviducts of recipient females. Twenty-seven (13.8% per transfer) cloned offspring were born by Caesarean section on day 19.5 and grew into adults. All offspring showed agouti coat color, as expected from the genotype of the donor cells. When they were examined for external genitalia by gross observation, one of the 27 clones seemed to be a female, with a vaginal opening and no penile structure (Fig. 1a and b). The remaining 26 clones were normal males in appearance. To determine whether this female-looking clone was behaviorally and functionally a female, we mated it with a male littermate. Within about five months, it gave birth to three litters (one, two, and five pups each; 4 females and 4 males). Thus, despite a low reproductive performance, it was a fertile female born after SCNT using a male mouse (Fig. 1c). We analyzed 10 chromosome spreads from tail-tip cells collected from the female clone. All spreads showed a 39,X karyotype, indicating that the clone was an XO female, resulting from the loss of the Y chromosome (Fig. 2).

Although a more detailed systemic karyotype analysis is required, we tentatively infer that the Y chromosome was deleted in the donor cell or at some early step during nuclear transfer. It is known that the Y chromosome can be lost in populations of cultured mouse embryonic stem (ES) cells and that such XO ES cells can give rise to female mice via chimeric embryo formation [10] or nuclear transfer [11, 12]. However, because we used the donor cells shortly after their collection from autopsied mice, it is very unlikely that the *in vitro* manipulation of the donor cells caused the loss of the Y chromosome. As far as we know, there is no information available about how often XO cells are generated in a male body, but some may survive *in situ* because no essential genes are coded on the Y chromosome. Although the sex-reversed SCNT in our case was accidental, theoretically, we may be able to produce female clones from donor male animals if it becomes possible to

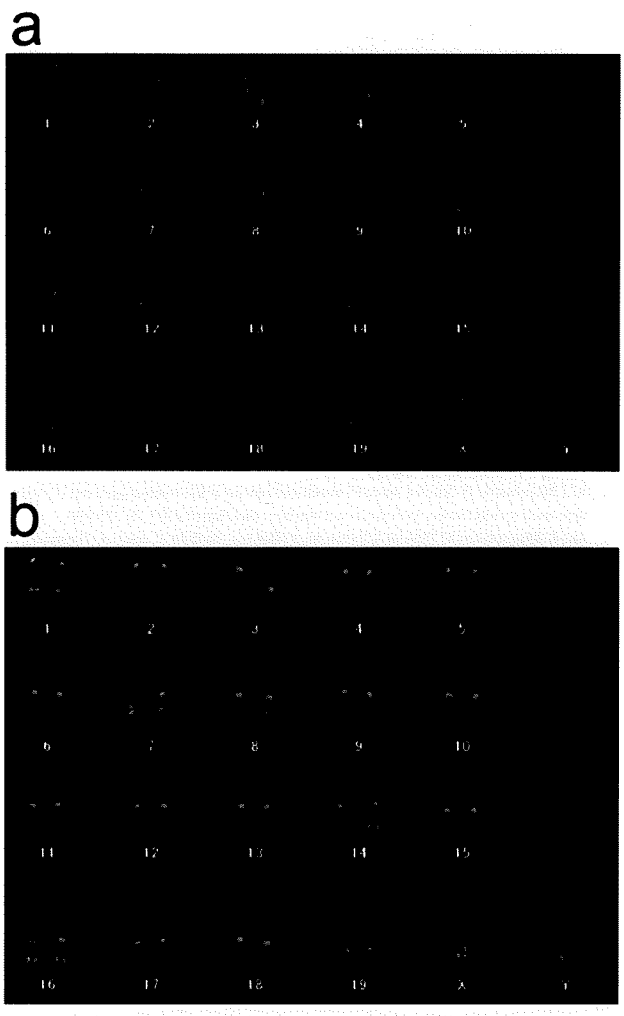

Fig. 2. Chromosome spreads from fibroblast cells from the female cloned from a Sertoli cell (a) and a male mouse (b). The 39 chromosome pairs and the absence of the Y chromosome in (a) indicate that it is an XO female.

sort XO cells from a suspension of male cells. Alternatively, establishment of ES cells from SCNT embryos may allow production of cloned XO females because ES cells facilitate *in vitro* genetic manipulation and increase SCNT efficiency. At present, nuclear-transferred ES cells can be generated efficiently only in mice [13], but recent significant improvements in controlling cell-autonomous pluripotency may allow the establishment of ES cells in other species [14, 15].

Another issue that should be considered in SCNT with XO cells is the normality of the resulting cloned females. In humans, the XO karyotype can arise from incomplete chromosomal segregation [16] and often results in the development of Turner syndrome, which is associated with various developmental, endocrine, cardiovascular, psychosocial and reproductive abnormalities [17]. Most (>95%) patients are infertile because of ovarian dysfunction. In contrast, XO female mice are anatomically normal and fertile [18], although they often show developmental retardation [19, 20]. This species-specific difference may arise from differences in the sensitivity of some X-linked genes to haploinsufficiency. The human *RPS4* (ribosomal protein S4) gene is responsible for the onset of Turner syndrome because it is biallelically expressed under normal conditions [21]. In contrast, its mouse homologue, *Rps4*, is a gene subject to X chromosome inactivation, and its function is assured by the presence of a single allele [22]. Little information about the occurrence of XO females is available for other species, but the laboratory mouse is not the only species known to produce normal XO females. A very few XO female shrews have been captured in their natural habitats [23].

If sex-reversed SCNT becomes available, it is expected to be most effectively used for production of offspring from very limited genetic resources. Recently, several lines of evidence have shown that the genetic integrity of somatic cells is more resistant to freezing processes than previously thought. Even after freezing without cryoprotectants [24], freeze-drying [25, 26] or freezing in intact bodies or organs for many years [4, 5], the nuclei of these dead cells retain their ability to support full-term development when transferred into enucleated oocytes. Therefore, we can speculate that, with this approach, we can rescue endangered species or resurrect animals that have already disappeared. However, SCNT is asexual reproduction and is expected to produce only animals of the donor sex. Although significant technical advances are required and inbreeding depression may become another issue, our finding clearly indicates the possibility that sexual reproduction may be resumed after the donor cells are cloned from one male animal. Our finding might provide a potential new reproductive technology for the rescue or maintenance of wild animals in the future.

Acknowledgments

The donor mouse strain (RBRC 01260) was provided by the RIKEN BRC through the National BioResource Project of the Ministry of Education, Culture, Sports, Science and Technology (MEXT), Japan. This research was supported by grants from MEXT (KI, NO, AO), the Mochida Memorial Foundation for Medical and Pharmaceutical Research (KI), the Sumitomo Foundation (KI) and the NOVARTIS Foundation (Japan) for the Promotion of Science (KI).

References

1. **Yang X, Smith SL, Tian XC, Lewin HA, Renard JP, Wakayama T.** Nuclear reprogramming of cloned embryos and its implications for therapeutic cloning. *Nat Genet* 2007; 39: 295–302.
2. **Kishigami S, Mizutani E, Ohta H, Hikichi T, Thuan NV, Wakayama S, Bui HT, Wakayama T.** Significant improvement of mouse cloning technique by treatment with trichostatin A after somatic nuclear transfer. *Biochem Biophys Res Commun* 2006; 340: 183–189.
3. **Rybouchkin A, Kato Y, Tsunoda Y.** Role of histone acetylation in reprogramming of somatic nuclei following nuclear transfer. *Biol Reprod* 2006; 74: 1083–1089.
4. **Wakayama S, Ohta H, Hikichi T, Mizutani E, Iwaki T, Kanagawa O, Wakayama T.** Production of healthy cloned mice from bodies frozen at –20 C for 16 years. *Proc Natl Acad Sci USA* 2008; 105: 17318–17322.
5. **Hoshino Y, Hayashi N, Taniguchi S, Kobayashi N, Sakai K, Otani T, Iritani A,**

Saeki K. Resurrection of a bull by cloning from organs frozen without cryoprotectant in a –80 C freezer for a decade. *PLoS ONE* 2009; 4: e4142.

6. **Sado T, Hoki Y, Sasaki H.** *Tsix* silences *Xist* through modification of chromatin structure. *Dev Cell* 2005; 9: 159–165.
7. **Inoue K, Ogonuki N, Mochida K, Yamamoto Y, Takano K, Kohda T, Ishino F, Ogura A.** Effects of donor cell type and genotype on the efficiency of mouse somatic cell cloning. *Biol Reprod* 2003; 69: 1394–1400.
8. **Wakayama T, Perry AC, Zuccotti M, Johnson KR, Yanagimachi R.** Full-term development of mice from enucleated oocytes injected with cumulus cell nuclei. *Nature* 1998; 394: 369–374.
9. **Yoshida MC, Ikeuchi T, Sakai M.** Differential staining of parental chromosomes in interspecific cell hybrids with a combined quinacrine and 33258 Hoechst technique. *Proc Japan Acad* 1975; 51: 184–187.
10. **Sugawara A, Goto K, Sotomaru Y, Sofuni T, Ito T.** Current status of chromosomal abnormalities in mouse embryonic stem cell lines used in Japan. *Comp Med* 2006; 56: 31–34.
11. **Ono Y, Shimozawa N, Muguruma K, Kimoto S, Hioki K, Tachibana M, Shinkai Y, Ito M, Kono T.** Production of cloned mice from embryonic stem cells arrested at metaphase. *Reproduction* 2001; 122: 731–736.
12. **Shimozawa N, Ono Y, Muguruma K, Hioki K, Araki Y, Shinkai Y, Kono T, Ito M.** Direct production of gene-targeted mice from ES cells by nuclear transfer and gene transmission to their progeny. *Exp Anim* 2002; 51: 375–381.
13. **Wakayama T, Tabar V, Rodriguez I, Perry AC, Studer L, Mombaerts P.** Differentiation of embryonic stem cell lines generated from adult somatic cells by nuclear transfer. *Science* 2001; 292: 740–743.
14. **Buehr M, Meek S, Blair K, Yang J, Ure J, Silva J, McLay R, Hall J, Ying QL, Smith A.** Capture of authentic embryonic stem cells from rat blastocysts. *Cell* 2008; 135: 1287–1298.
15. **Li P, Tong C, Mehrian-Shai R, Jia L, Wu N, Yan Y, Maxson RE, Schulze EN, Song H, Hsieh CL, Pera MF, Ying QL.** Germline competent embryonic stem cells derived from rat blastocysts. *Cell* 2008; 135: 1299–1310.
16. **Hall H, Hunt P, Hassold T.** Meiosis and sex chromosome aneuploidy: how meiotic errors cause aneuploidy; how aneuploidy causes meiotic errors. *Curr Opin Genet Dev* 2006; 16: 323–329.
17. **Bondy CA.** Heart disease in Turner syndrome. *Minerva Endocrinol* 2007; 32: 245–261.
18. **Russell WL, Russell LB, Grower JS.** Exceptional inheritance of a sex-linked gene in the mouse explained on the basis that the X/O sex-chromosome constitution is female. *Proc Natl Acad Sci USA* 1959; 45: 554–560.
19. **Banzai M, Omoe K, Ishikawa H, Endo A.** Viability, development and incidence of chromosome anomalies of preimplantation embryos from XO mice. *Cytogenet Cell Genet* 1995; 70: 273–277.
20. **Burgoyne PS, Evans EP, Holland K.** XO monosomy is associated with reduced birthweight and lowered weight gain in the mouse. *J Reprod Fertil* 1983; 68: 381–385.
21. **Watanabe M, Zinn AR, Page DC, Nishimoto T.** Functional equivalence of human X- and Y-encoded isoforms of ribosomal protein S4 consistent with a role in Turner syndrome. *Nat Genet* 1993; 4: 268–271.
22. **Omoe K, Endo A.** Expression level of Rps4 mRNA in 39,X mice and 40,XX mice. *Cytogenet Cell Genet* 1994; 67: 52–54.
23. **Searle JB, Jones RM.** Sex chromosome aneuploidy in wild small mammals. *Cytogenet Genome Res* 2002; 96: 239–243.
24. **Li J Mombaerts P.** Nuclear transfer-mediated rescue of the nuclear genome of nonviable mouse cells frozen without cryoprotectant. *Biol Reprod* 2008; 79: 588–593.
25. **Loi P, Matsukawa K, Ptak G, Clinton M, Fulka J Jr, Nathan Y, Arav A.** Freeze-dried somatic cells direct embryonic development after nuclear transfer. *PLoS ONE* 2008; 3: e2978.
26. **Ono T, Mizutani E, Li C, Wakayama T.** Nuclear transfer preserves the nuclear genome of freeze-dried mouse cells. *J Reprod Dev* 2008; 54: 486–491.